[5] M. Atoji and W. N. Lipscomb, J. Chem. Phys. **27,** 195 (1957).
[6] C. Spenser and W. N. Lipscomb, J. Chem. Phys. **28,** 355 (1958).
[7] R. J. H. Clark and B. K. Hunter, J. Chem. Soc. A **1971,** 2999.
[8] J. J. Comeford, S. Abramowitz, and I. W. Levin, J. Chem. Phys. **43,** 4536 (1965).
[9] M. A. Rollier and A. Riva, Gazz. Chim. Ital. **77,** 361 (1947).
[10] A similar conclusion has previously been reached from NQR results; see W. G. Laurita and W. S. Koski, J. Am. Chem. Soc. **81,** 3179 (1959).
[11] M. A. Ring, J. D. H. Donnay, and W. S. Koski, Inorg. Chem. **1,** 109 (1962).
[12] This assignment for ν_2 has been proposed previously; see A. Finch, I. J. Hyams, and D. Steele, Trans. Faraday Soc. **61,** 398 (1965). However, their spectra were unsatifactory, in particular with respect to the considerable infrared activity of ν_1 (forbidden by selection rules), and the unlikely values suggested for $2\nu_4$. Either complex formation between the triiodide and the solvent (carbon disulfide or benzene) or partial decomposition may have taken place.
[13] D. C. McKean, J. Chem. Phys. **24,** 1002 (1956).
[14] I. W. Levin and S. Abramowitz, J. Chem. Phys. **43,** 4213 (1965).
[15] D. A. Dows, *Physics and Chemistry of the Organic Solid State,* edited by D. Fox, M. M. Labes, and A. Weissburger (Interscience, New York, 1963), Chap. II, p. 657.
[16] D. F. Hornig, Discussions Faraday Soc. **9,** 115 (1950).

THE JOURNAL OF CHEMICAL PHYSICS VOLUME 56, NUMBER 5 1 MARCH 1972

Exact and Approximate Quantum Mechanical Reaction Probabilities and Rate Constants for the Collinear $H+H_2$ Reaction*

DONALD G. TRUHLAR† AND ARON KUPPERMANN
A. A. Noyes Laboratory of Chemical Physics,‡ California Institute of Technology, Pasadena, California 91109
(Received 13 September 1971)

We present numerical quantum mechanical scattering calculations for the collinear $H+H_2$ reaction on a realistic potential energy surface with an 0.424 eV (9.8 kcal) potential energy barrier. The reaction probabilities and rate constants are believed to be accurate to within 2% or better. The calculations are used to test the approximate theories of chemical dynamics. The reaction probabilities for ground vibrational state reagents agree well with the vibrationally adiabatic theory for energies below the lowest threshold for vibrational excitation, except when the reaction probability is less than about 0.1. For these low reaction probabilities no simple one-mathematical dimensional theory gives accurate results. These low reaction probabilities occur at low energy and are important for thermal reactions at low temperatures. Thus, transition state theory is very inaccurate at these low temperatures. However, it is accurate within 40% in the higher temperature range 450–1250°K. The reaction probabilities for hot atom collisions of ground vibrational state reagents with translational energies in the range 0.58 to 0.95 eV agree qualitatively with the predictions of the statistical phase space theory. For vibrationally excited reagents the vibrational adiabatic theory is not accurate as for ground vibrational state reagents. The lowest translational energy of vibrationally excited reagents above which statistical behavior manifests itself is less than 1.0 eV.

I. INTRODUCTION

Recent advances in the application of computer-based numerical methods to quantum mechanical problems of chemical interest have made possible accurate solutions of the internuclear motion scattering problem for many nonreactive collisions. Reactive collisions are more complicated and essentially exact solutions have only been obtained by reducing the dimensionality of the problem,[1–5] e.g., by considering purely collinear collisions.[1,3–6] Some studies have also been carried out for collinear nonreactive collisions and for collinear reactive model problems with unrealistic potential surfaces. In all cases that accurate numerical solutions have been obtained for the internuclear motion scattering problem, they are for an assumed potential energy surface. The $H+H_2$ reaction is a prototype case for studies of this type for several reasons: (1) the electronic energy problem can be solved more accurately than for most other reactions, engendering some confidence in the potential energy assumed to govern the internuclear motion; (2) excited electronic states are higher in energy in this case than for most other reactions, minimizing the error introduced by assuming the scattering to occur on one unique potential energy surface; (3) the atoms are light so that interesting quantum effects are expected to show up more clearly than for most other reactions. In this paper we report the exact solution of the scattering problem for the collinear $H+H_2$ reaction for an approximate but realistic representation of the potential energy surface. However, the nuclear wavefunctions were not made antisymmetric with respect to interchange of identical nuclei, and thus effects associated to such antisymmetrization are not included. Similar calculations were performed by Mortensen and Pitzer[1] and Mortensen and Gucwa[3] but were limited to a smaller energy range (relative translational energies from 0.14 to 0.34 eV plus a point at 0.49 eV) than that considered here (relative translational energies from 0.005 to 1.22 eV). McCollough and Wyatt[7] have presented some results from an exact treatment in a time-dependent formulation. In that formulation the wave packet includes particles with a distribution of energies. Their results are at comparatively low energy. We have published a preliminary report of the first exact calculations for

this system in which excited vibrational levels became important.[4] The present paper is an extension of that work. Since then, Diestler[5] has published close-coupling calculations for the collinear $H+H_2$ reaction for energies at which the first excited state of the reaction product is accessible.

In general, calculations on collinear collisions cannot be directly compared with experiment (in a few cases they can be considered as an approximate treatment of back-scattering collisions and compared to large-angle scattering experiments). Their main interest is that they can provide an exact solution of a well-defined model problem incorporating a realistic potential energy surface. This exact solution can be compared to approximate ones of the same model to test and evaluate the approximate methods which are often applied to real problems. In addition, the exact solution of the realistic model problem is of intrinsic interest in that it is a detailed chemical experiment which cannot be performed in the laboratory. In this paper we test several such approximate methods against the exact solution. These methods include transition state theory,[8–20] the statistical theory of reactions with an energy barrier,[21–22] and the vibrationally adiabatic theory of reactions.[23–27]

It will be interesting when many other approximate theories are compared to these exact results in the future. The most accurate treatment of the $H+H_2$ reaction in three dimensions has been the approximate distorted wave treatment of Karplus and Tang.[28] (Their calculations were for relative translational energies of 0.25–3.3 eV). It would, therefore, be interesting to compare the distorted wave theory for the collinear reaction to the exact results reported here.

In Sec. II we present our potential energy surface. In Sec. III we discuss the method used to solve the Schrödinger equation and to compute exact reaction probabilities and rate constants. Section IV discusses the calculations using the approximate methods. In Sec. V we present the results of our exact calculations. In Sec. VI we discuss these results and compare them with the approximate methods. Section VII is a summary of important conclusions.

II. POTENTIAL ENERGY SURFACE

The $H+H_2$ reaction at energies up to a few electron volts proceeds in the ground electronic state with the nuclear motion determined by an effective potential which can be calculated using the Born–Oppenheimer separation of electronic and internuclear motions. This potential has been calculated fairly accurately (using configuration interaction techniques to solve for the electronic wavefunctions) by Shavitt, Stevens, Minn, and Karplus (SSMK).[29] Their results confirm the conclusion from many earlier less accurate *ab initio* calculations, that the lowest energy reaction path for the $H+H_2$ reaction corresponds to a linear collision and that the highest potential energy that must be achieved along this minimum energy path (or reaction path) occurs for the symmetrical configuration where the two bond lengths are equal ($R_{AB}=R_{BC}$ in the notation of Sec. III.A.2). Their calculation predicts that this barrier height E^b is 0.477 eV. Shavitt[19] estimated that the best guess at the real barrier, as determined by comparing transition state theory to the rate experiments of Westenberg and de Haas[17] and others, is 0.424 eV. He suggested that the barrier in the SSMK surface be scaled by a factor $(0.424/0.477)=0.89$ along the entire reaction path but that the predicted energy variation not be scaled in directions transverse to this minimum energy path. His suggested scaling can be applied in a straightforward way at the barrier top (which is the saddle point of the potential energy surface), but is purposefully ambiguous at other places because transition state theory calculations depend mainly on the region around the barrier top. In the $H+H_2$ reaction there is a long range potential due to the induced dipole–induced dipole dispersion interaction. This long range interaction produces a shallow potential well in the surface at large separation of H and H_2. The depth and shape of this well are not known accurately; however, an estimate which is probably accurate within a factor of 2 of the depth is the value of 0.001 eV obtained from the SSMK calculations.[29] The approximate calculations of Dalgarno, Henry, and Roberts also predict a potential well depth of 0.001 eV.[30] This depth is more than a factor of a hundred less than almost all the translational energies in which we are interested here for reactive collisions. It is thus not expected to have a significant effect on the scattering considered here and we will neglect it.

It is convenient for carrying out the scattering calculations to have an analytic representation of the potential energy as a function of the internuclear distances involved. Shavitt *et al.* fit their surface for linear collisions to an expression with 28 linear parameters and one nonlinear parameter.[29] This is a fit to the surface before scaling. If we consider only collinear collisions, one way to generalize the scaling suggested by Shavitt to the whole surface is by adopting a procedure developed by Wall and Porter for constructing parametrized potential energy surfaces.[31] This method can be used to construct a surface which has the scaled barrier height, the transition state parameters suggested by Shavitt[19] (as discussed above these are the parameters of the SSMK surface except in the direction of the reaction coordinate), and the correct asymptotic H_2 behavior in the separated atom plus diatom limit. In addition the method still has one as yet undetermined parameter (l in the notation of Wall and Porter). The effect of this parameter is to change the position of the minimum energy reaction path. It turns out that this parameter *can* be chosen so that the contours of the Wall–Porter-type surface (with barrier height 0.424 eV) are approximately parallel all over the surface to the contours for the SSMK surface

TABLE I. Potential energy surface parameters.

$D=4.7453$ eV
$a=0.08939$
$l=3$
$s_0=1.765a_0$
$\alpha^{\ddagger}=0.70152a_0^{-1}$
$\alpha_0=1.04435a_0^{-1}$
$x_0=1.40083a_0$
$R_0=3.6213a_0$

with barrier height 0.477 eV. This choice yields $l=3$. Figure 1 is a comparison of the SSMK surface and the Wall–Porter parametrized surface with $l=3$ for the linear H_3 collision. If the shape of the accurate surface (the SSMK surface) had been such that none of the family of surfaces obtainable by the method of Wall and Porter could be made to resemble it, we would have had to use a different method to obtain an analytical representation of the surface.

The Wall–Porter-type fit with $l=3$ to the scaled SSMK surface will simply be called the scaled SSMK surface in the rest of this article. Table I lists all potential parameters (in the notation of Wall and Porter[31]) which are necessary to calculate the scaled SSMK surface.

III. METHOD FOR EXACT SCATTERING CALCULATIONS

A. Reaction Probabilities

To obtain the reaction probabilities as a function of energy, we use a time-independent formulation. Several methods have been proposed for the exact solution of this collinear collision atom–diatomic molecule rearrangement scattering problem.[2–4,6,32–35] In addition, there are other more general numerical methods which can be applied to this problem.[36–38] We used the finite-difference boundary-value method (FDBVM) of Diestler and McKoy (DM)[32] with some modifications described in this section. The FDBVM is similar to the finite difference method first applied to this problem by Mortensen and Pitzer.[2] The main difference is that the boundary conditions are imposed noniteratively in the FDBVM[32] and iteratively in the method used by Mortensen and Pitzer.[2,3]

1. Changes in the Method of Diestler and McKoy

For the analyses in the asymptotic region of the numerical solutions with arbitrary boundary conditions (χ's in the notation of Ref. 32), DM used a fixed (i.e., independent of step size) approximation to the exact eigenfunction for the vibrational potential well of the separated diatom. The integrals involving these functions were evaluated by Simpson's rule. These procedures are inconsistent with the numerical method (second differences) used by them and also here to obtain the χ's and they can lead to spurious results. For the analyses, we used numerical solutions for the eigenfunctions which are obtained with the same order finite difference approximation and the same step size h as used to compute the χ's. Integrals over these functions were evaluated using the trapezoidal rule. This is a consistent analysis. Further, when the results are extrapolated to $h=0$, the boundary values and the χ's both converge at equivalent rates to the exact values. In the method of DM, the χ's would converge to accurate solutions for inexact boundary values, i.e., to inexact solutions.

Diestler and McKoy extrapolated their approximate scattering probabilities $P(h_j)$ for four different values h_j of the step size by solving the equations

$$P(h_j)=\sum_{i=1}^{4} P_{i-1}h_j^{i-1}, \qquad j=1, 2, 3, 4 \qquad (1)$$

for the extrapolated scattering probability $P_0=P(0)$. It is well known that the local truncation error due to using the second central differences (the procedure used here) to approximate elliptic differential operators like those occurring in our problem can be expressed as a power series in h_j which includes only even powers.[39] Thus we performed extrapolations using

$$P(h_j)=\sum_{i=1}^{M} P_{i-1}h_j^{2(i-1)}, \qquad j=1, 2, \cdots, M \qquad (2)$$

where M varied from 2 to 7. (For the final results reported here we used $M=2$ or 3; see below.) By comparing several extrapolation methods with very accurate ones (obtained using finer grids and large M) in test cases, we found that (2) led to much more accurate and consistent results than (1) for this problem. Equation (1) may lead to large errors, evidently because the right hand side does not accurately represent the finite difference errors. Use of Eq. (2) with $M=2$ or

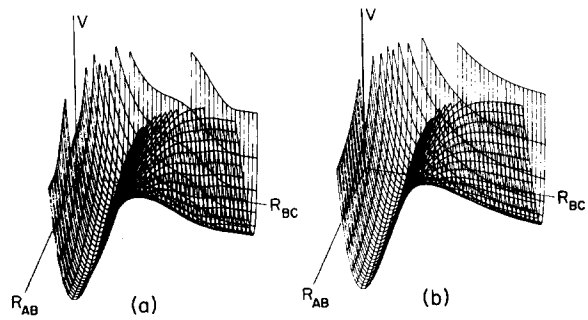

FIG. 1. Three-dimensional projection views (viewing angles: $\theta=53°$, $\phi=16°$) of: (a) scaled SSMK surface (scaled Wall–Porter type surface with $l=3$); (b) Shavitt–Stevens–Minn–Karplus H_3 surface. The vertical axis is potential energy, and the horizontal ones are the internuclear distances, as defined in Sec. III.A.2.

3 is called Richardson's h^2- or h^4-extrapolation, respectively.[40]

Diestler and McKoy analyzed their solutions in the asymptotic region in terms of traveling waves.[32] This is equivalent to analyzing the solutions directly for (complex) elements of the scattering matrix **S**. We analyzed our solutions in terms of standing waves. This procedure yields directly the (real) elements of the reactance matrix **R**. We can compute the scattering matrix from the reactance matrix by the well-known formula[41]

$$\mathbf{S}=(1-i\mathbf{R})^{-1}(1+i\mathbf{R}). \tag{3}$$

The analysis for the **R** matrix elements is presented in Appendix I. If one obtains a very accurate numerical solution, **S** and **R** computed by either method are automatically symmetric to several significant digits, **S** is automatically unitary to several digits, and **S** computed from **R** is equal to **S** computed directly. In less accurate calculations, **S** computed by the method of DM does not satisfy these properties. However, if we use the standing-wave analysis, we can introduce a symmetrized reactance matrix $\mathbf{R}^s$ whose elements are defined by

$$R_{ij}^s=\tfrac{1}{2}(R_{ij}+R_{ji}). \tag{4}$$

The scattering matrix computed using (3) and $\mathbf{R}^s$ is then unitary and symmetric (the well-known interpretation of these properties of the **S** matrix is that the calculation satisfies detailed balance and conservation of particle flux).[41] Accurately extrapolating to $h=0$ the **S** computed by either analysis scheme yields a unitary and symmetric **S**. The main advantage of using the symmetrized standing-wave analysis is that it is more convenient (because the reactance matrix elements are real and because the computed transition probabilities always automatically sum to 1.0) and the results are found to be more accurate for a given step size or set of step sizes (and thus for a given computing time) than for a direct traveling wave analysis. The latter property is interesting since Delves[42] showed for a similar scattering problem that the transformation (4) is a variational improvement over a nonsymmetrical approximate **R**. We continued to perform the traveling wave analysis for the purpose of providing an extra indication of the accuracy of our results, but used the symmetrized reactance matrix analysis for the results we report. Although we find better results using the standing wave analysis for the present calculations, involving a symmetrical reaction, one should be cautious about expecting such results in general.

Finally, our computer program used the generalized **R** and **T** matrices of Johnson and Secrest[1] to facilitate the handling of closed channels. This involves redefining some of the matrix elements involving closed channels so that the numbers are representable in the computer.

2. Details of the Numerical Work

We label the three H atoms A, B, and C, where B is the central one. Let R_{AB} and R_{BC} be the distances between atoms A and B and between atoms B and C, respectively. We solved numerically for the wavefunction in the square region bounded by the lines: $R_{AB}=0.3a_0$, $R_{BC}=0.3a_0$, $R_{AB}=4.2a_0$, $R_{BC}=4.2a_0$. Each numerical solution was assumed to vanish on the first two of these lines and one other; on the fourth it was taken to be one of the diatom numerical eigenfunctions obtained as outlined in Sec. III.A.1 above.

For a given energy and step size where N'' reagent plus product channels are open (in the notation of Appendix II), we obtained $N''+6$ numerical solutions in terms of which to expand the wavefunction. In the energy range considered here this means we used 8 to 12 linearly independent χ's in each case.

The analysis of the χ's was carried out in each of the two asymptotic regions in terms of all the open channels plus at least the next four channels (the first four closed channels) in that asymptotic region; thus usually five to seven channels in each asymptotic region were kept for analysis.

The step sizes used for individual (unextrapolated) runs were in the range $h=0.111$–$0.051a_0$. The calculations correspond to the solution of 1156–5625 simultaneous linear equations. The symmetric finite difference matrices are banded with bandwidths of 69–151.

The accuracy of reaction probabilities calculated using these procedures was estimated by studying the effect of varying each of the parameters of the numerical method. All these parameters were fixed at values such that the predominant numerical error is that due to the finite step size. This error was estimated by comparing results extrapolated from different sets of runs using different step sizes. This procedure indicates that the results presented here are accurate within 2% or better, generally better. We will refer to these reaction probabilities as the exact ones.

An example showing the degree of symmetry of the reactance, scattering and probability matrices for a case where Eq. (4) is not applied is given in Appendix II and Table IX, which also shows the probability matrix obtained from this equation.

B. Rate Constants

In one dimension, the rate of the bimolecular reaction A+BC→AB+C is

$$d[\mathrm{A}]/dt=d[\mathrm{BC}]/dt=-k_r[\mathrm{A}][\mathrm{BC}], \tag{5}$$

where [A] and [B] are concentrations in molecules/cm and k_r is the rate constant in centimeters per molecule per second. By a procedure analogous to that used by Eliason and Hirschfelder[43] in the three-dimensional case, it is easily shown that for BC in the nth vibrational state and a thermal distribution of relative translational

energies the rate constant is

$$k_r(n, T) = (2\pi\mu kT)^{-1/2} \int_0^\infty P_n(E_n) \times \exp(-E_n/kT)\, dE_n, \quad (6)$$

where k is Boltzmann's constant, T is the absolute temperature, $P_n(E_n)$ is the probability of reaction when the molecule is in state n with initial relative translational energy E_n, and

$$\mu = M_A M_{BC}/(M_A + M_{BC}) \quad (7)$$

is the reduced mass of the A+BC system. For a thermal distribution of initial vibrational levels the rate constant is

$$k_r(T) = \sum_n k_r(n, T)\, p_n(T), \quad (8)$$

where

$$p_n(T) = (Q^v)^{-1} \exp[-(E_n{}^v - E_0{}^v)/kT] \quad (9)$$

is the fraction of reagent molecules in vibrational state n, $E_n{}^v$ is the corresponding vibrational energy level, and Q^v is the vibrational partition function (computed with the zero of energy at the zero point energy of the reactants).

The integral in Eq. (6) was evaluated accurately by two different numerical methods. The rates $k_r(n, T)$ and $k_r(T)$ will be called the exact rate constants.

C. Tunneling Corrections

The usual method of calculating transition state theory (TST) rate constants is to calculate a rate $k_0{}^{TST}$ assuming that the motion along the reaction path is classical and to calculate a quantum correction κ_1 such that the actual TST rate constant is

$$k^{TST}(T) = \kappa_1(T)\, k_0{}^{TST}(T). \quad (10)$$

An expression for $k_0{}^{TST}(T)$ is given by Eq. (24) below. We shall follow the usual convention of calling κ_1 a tunneling correction. It is also sometimes called the transmission coefficient. It is usually assumed that a separable reaction coordinate exists and κ_1 is computed as an approximate[13–16,18,19] or exact[20,44,45] quantum mechanical correction to a classical treatment of motion along that coordinate. The potential energy as a function of distance along the reaction coordinate is a barrier of height $E_0{}^b$ and thus

$$\kappa_1(T) = \int_0^\infty T_1(E_0) e^{-E_0/kT} dE_0 \Big/ \int_0^\infty T_1{}^{cl}(E_0)\, e^{-E_0/kT} dE_0, \quad (11)$$

where $T_1(E_0)$ is the quantum mechanical transmission probability for the one-dimensional problem at translational energy E_0. $T_1{}^{cl}(E_0)$ is the classical transmission probability for the one-dimensional problem, equal to 0 for $E_0 < E_0{}^b$ and 1 otherwise. The problem of how the one-dimensional potential function for motion along the reaction coordinate is related to the multidimensional potential energy surface has been discussed elsewhere.[16,45,46] In general one of the following two models has been used: (1) conservation of vibrational energy approximation (CVE), in which the barrier is the classical potential energy along the reaction path and $E_0{}^b = E_b$; (2) vibrational adiabaticity approximation with no correction for reaction path curvature (called VA in Ref. 45 but VAZC here to emphasize that the zero-curvature approximation[46] for the reaction path has an effect on the barrier; this is discussed further in Sec. IV.B) in which the local vibrational energy is assumed to adjust adiabatically along the reaction path (i.e., the vibrational quantum number in the direction transverse to the reaction path is conserved) and this change modifies the effective potential energy for one dimensional motion along the reaction path. In the latter case, the barrier $E_0{}^b$ is

$$E_0{}^{VAZC} = E_b + E_0{}^{vs} - E_0{}^v, \quad (12)$$

where $E_0{}^{vs}$ and $E_0{}^v$ are the zero point energies associated with the symmetric stretching vibration of the classical transition state and the diatomic vibration, respectively.

It is possible to modify the definition of the tunneling correction. For example, we can define an extended tunneling correction by

$$k^{TST}(T) = \kappa_2(T)\, k_0{}^{TST}(T), \quad (13)$$

where

$$\kappa_2(T) = \frac{\int_0^\infty T_2(E_0) \exp\left(-\frac{E_0}{kT}\right) dE_0}{\int_0^\infty T_1{}^{cl}(E_0) \exp\left(-\frac{E_0}{kT}\right) dE_0} = (2\pi\mu/kT)^{1/2} \exp(E_0{}^b/kT)\, k_r(0, T), \quad (14)$$

in which $T_2(E_0)$ is the exact reaction probability for the two-mathematical-dimensional treatment of the collinear reaction. This definition, however, assumes knowledge of $T_2(E_0) = P_0(E_0)$. Under these conditions, $k_r(0, T)$ can be obtained exactly from (6) and TST would not be necessary. This further implies that $P_n(E_n)$ is obtainable and hence that $k_r(T)$ can be obtained from Eq. (8) rather than from TST.

Just as for the one-dimensional tunneling treatments, there are various possible choices of $E_0{}^b$ which correspond to different models of the reaction. The choice (12) is most consistent with the adiabatic derivation of transition state theory,[45] and our results given in Sec. IV show the choice $E_0{}^b = E_0{}^{VAZC}$ leads to more consistent results than $E_0{}^b = E_b$.

Another definition of the tunneling correction was given by Mortensen.[3] He defined the transmission coefficient as

$$\kappa_e(T) = k_r(T)/k_0{}^{TST}(T), \quad (15)$$

where the numerator is the exact rate constant [Eq. (8)] and the denominator is that calculated by transition state theory without tunneling [Eq. (24)]. This definition will be considered again in Sec. VI.H.

IV. METHODS FOR APPROXIMATE SCATTERING CALCULATIONS

A. Statistical Theory

The statistical phase space theory in a classical mechanical version was applied to the three-dimensional H+H$_2$ reaction by Lin and Light.[21] This application involved postulating a requirement for strong-coupling collisions in terms of an energy barrier E_A^0. We now formulate their theory for one-dimensional collisions in a quantum mechanical form. We use the same energy barrier requirement as postulated by them. Let $P(n, E_n; m)$ be the probability of the molecule in a state n with relative translational energy E_n and vibrational energy E_n^v reacting to produce product in state m. Then

$$P(n, E_n; m) = [N(E_T)]^{-1} \tag{16}$$

with

$$E_T = E_n + E_n^v, \tag{17}$$

$$N(E_T) = \sum_i h(i, E_T), \tag{18}$$

$$h(i, E_T) = 1 \quad \text{for } (E_T - E_i^v) \geq E_A(i)$$
$$= 0 \quad \text{otherwise}, \tag{19}$$

$$E_A(i) = \max \begin{Bmatrix} E_A^0 - \lambda_v E_i^v \\ 0 \end{Bmatrix}. \tag{20}$$

Equation (20) shows that E_A^0 is the energy barrier to reaction if vibrational energy does not contribute, and λ_v is the fraction of vibrational energy which contributes to overcoming the barrier. Equation (18) gives the total number of open channels which are strongly coupled to one another when the total energy is E_T. Lin and Light assumed $E_A^0 = 0.368$ eV and $\lambda_v = 1$ for their treatment of the three-dimensional H+H$_2$ reaction.

B. Vibrationally Adiabatic Theory

According to the vibrationally adiabatic theory of reactions,[23–25] the initial vibrational quantum of BC is adiabatically transformed to a quantum of symmetric stretching vibration of ABC at the transition state, and finally to a quantum of AB vibration in the product. Thus the vibrational quantum number does not change, and

$$P(n, E_n; m) = \delta_{mn} T_1(E_n, n), \tag{21}$$

where δ_{mn} is the Kronecker delta and $T_1(E_n, n)$ is the probability of transmission for the one-dimensional vibrationally adiabatic (VA) barrier. This barrier has been discussed quantitatively elsewhere.[45–50] For the present study, we calculated the VA barrier for the scaled SSMK surface by finding the reaction path in normal coordinate space, and calculating for many points along it the one-dimensional vibrational energy of quantum state n in the direction perpendicular to the reaction path. This local transverse vibrational energy was added to the potential energy at each of those points to give the effective potential energy for one-dimensional motion along the reaction path in the VA approximation for vibrational quantum state n. This technique has been discussed in more detail previously.[45] In the calculation of this barrier we made the harmonic approximation for the vibrations. We then calculated transmission across this barrier in the Cartesian approximation, i.e., we straighten the barrier out and do a calculation in one Cartesian coordinate. This is an approximation since the actual reaction path is quite curved near the saddle point on the potential energy surface.[19,45]

TABLE II. Vibrational energies of reactants E_n^v and transition state E_n^{vs} and vibrationally adiabatic energy barriers E_n^{VAZC}.[a]

n	E_n^v (eV)	E_n^{vs} (eV)	E_n^{VAZC} (eV)
0	0.2728	0.5487	0.2759
1	0.7940	0.7923	−0.0017
2	1.2830	1.0287	−0.2543
3	1.7397	1.2577	−0.4820
4	2.1641	1.4793	−0.6848
5	2.5562	1.6936	−0.8626

[a] Calculated by a finite difference boundary value method and h^4 extrapolation (see Eq. 2) using 55, 65, and 75 grid points and same boundaries as for scattering calculation.

We have thus excluded corrections for reaction path curvature in normal-coordinate space from both the computation of the transverse vibrational energy and from the one-dimensional barrier transmission calculation. Our VA model is thus entirely equivalent to the one Wyatt has called[46] the zero-curvature (ZC) approximation and we will refer to it as the vibrationally adiabatic zero-curvature approximation (VAZC). In the terminology of Marcus[50] we are assuming the reaction coordinate is Cartesian and are neglecting curvilinear-reaction-coordinate effects.

We consider two approximations to this motion along the reaction path: (1) classical

$$T_1^{cl}(E_n, n) = 0 \quad \text{for } E_n < E_n^{VAZC}$$
$$= 1 \quad \text{otherwise}, \tag{22}$$

where E_n is the relative reagent translational energy for BC in vibrational state n and E^{VAZC} is the corresponding VAZC barrier height

$$E_n^{VAZC} = E_b + E_n^{vs} - E_n^v. \tag{23}$$

Here E_n^{vs} is the energy of the transition state sym-

TABLE III. 1-MD potential energy barrier parameters [Eq. (28)].

	Barrier	
	VAZC	CVEZC
B (eV)	0.2772	0.4242
b_1 (eV)	0.2982	0.2691
b_2 (eV)	−0.0224	0.0[a]
b_3 (a_0^{-2})	0.94185	1.01006
b_4 (a_0^{-2})	0.11655	1.16372

[a] Not optimized.

metric stretching vibration in quantum state n; (2) quantum mechanical, in which case $T_1(E_n, n)$ is the exact solution of the one-dimensional quantum mechanical barrier transmission problem. The numerical solution of such a one-dimensional problem has been considered previously.[45]

The vibrational energy levels of the reactants and the transition state are given in Table II. They were obtained by a numerical solution of the appropriate vibrational eigenvalue equation. For the ground vibrational state, this gives a VAZC barrier height of 0.276 eV, which is 0.001 eV less than that obtained using a harmonic approximation to the corresponding potentials. This provides some justification for using this approximation in the calculation of the whole VAZC barrier. This barrier for the ground vibrational state (see Fig. 2) is rather flat over a large region (about $0.4a_0$ long) near the classical transition state. This flat shape is also apparent in a vibrationally adiabatic barrier calculated by Child for the lowest vibrational–rotational state in a zero angular momentum collision of H+H_2 in a plane.[48] (Child does not give the full details of his calculation).

C. Transition State Theory

In transition state theory the one-dimensional rate constant is given by Eq. (10) or (13) with[2]

$$k_0^{\mathrm{TST}}(T) = (kT/h)\,(Q^{vs}/Q^{\mathrm{rel}}Q^{v})\,\exp(-E_0^{\mathrm{VAZC}}/kT), \tag{24}$$

where Q^{v} was defined in Eq. (9), Q^{rel} is the relative motion translational partition function per unit length, and Q^{vs} is the partition function of the symmetric stretching vibration of the transition state (computed with the zero of energy at the zero point energy level of the classical transition state). Using the energy levels in Table II we computed Q^{v} and Q^{vs} by direct summation. Using methods published previously[45] we also computed the one-dimensional tunneling correction of Eq. (11) numerically for the scaled SSMK surface in both the CVE and VAZC approximations. (Since we make the zero-curvature assumption for the reaction path in all the one-dimensional barrier calculations, the transmission probability computed from the CVE barrier will henceforth be denoted CVEZC.) These corrections $\kappa_1^{\mathrm{CVEZC}}$ and κ_1^{VAZC} can be used to calculate the transition state theory rate constants

$$k_1^{\mathrm{CVEZC}}(T) = \kappa_1^{\mathrm{CVEZC}}(T)\,k_0^{\mathrm{TST}}(T) \tag{25}$$

and

$$k_1^{\mathrm{VAZC}}(T) = \kappa_1^{\mathrm{VAZC}}(T)\,k_0^{\mathrm{TST}}(T). \tag{26}$$

We will not consider any transition state theory treatments that do not assume zero curvature. Eq. (26) is the usual method[13–15,19] of calculating transition state theory rate constants except that we do not here assume an approximate method (such as that of Bell[51] or Eckart[52]) to compute $\kappa_1^{\mathrm{CVEZC}}$. Equation (26) is the method which is more consistent with the VA derivation of transition state theory.[45]

In performing the 1-MD tunneling calculations for Eqs. (25) and (26) the barriers are represented analytically by nonlinear least squares fits of the form

$$V(s) = b_1\,\mathrm{sech}^2(b_3 s^2) + b_2\,\exp(-b_4 s^2) + (B - b_1 - b_2)\,\exp(-4b^4 s^2), \tag{27}$$

where s is the distance from the barrier maximum. The parameters are given in Table III. This representation agrees with the actual barriers to within 0.004 eV over most of the range of the reaction coordinate.

We also use Eq. (14) with $E_0^b = E_b$ to compute κ_2^{CVE} and with $E_0^b = E_0^{\mathrm{VAZC}}$ to compute κ_2^{VAZC}. Then we calculate the extended transition state theory rate constants

$$k_2^{\mathrm{CVE}}(T) = \kappa_2^{\mathrm{CVE}}(T)\,k_0^{\mathrm{TST}}(T) \tag{28}$$

and

$$k_2^{\mathrm{VAZC}}(T) = \kappa_2^{\mathrm{VAZC}}(T)\,k_0^{\mathrm{TST}}(T). \tag{29}$$

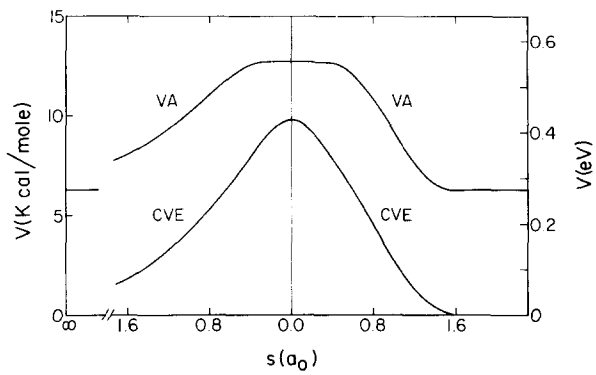

FIG. 2. Potential energy barriers for the collinear H+H_2 reaction as functions of distance s (in the normal-coordinate space of Refs. 19 and 45) along the reaction path from the saddle point of the surface. The barriers are symmetric about $s=0$ so only half of each barrier is shown. The CVE barrier is the classical conservation-of-vibrational-energy barrier. The VA one is the one obtained by assuming vibrational adiabaticity. Both barriers involve the zero-curvature assumption. The barriers on the right are the ones obtained from the potential energy surface of this article. The ones on the left are the more accurate barriers of Ref. 45. The barriers on the left are not part of any potential energy surface defined for R_{AB}, R_{BC} off the reaction coordinate, however.

TABLE IV. Rate constants from exact calculations [$k_r(T)$] compared with those from transition state theory [$k_{TST}(T)$].[a]

	$k_{TST}(T)$ [b]						
T (°K)	κ_1^{CVEZC}	κ_1^{ECVEZC}	κ_2^{CVE}	$\kappa^{el}=1$	κ_1^{VAZC}	κ_2^{VA}	$k_r(T)$
200	2.15(0)	4.66(0)	1.24(3)	6.99(−3)	1.20(−2)	2.44(−1)	2.07(−1)
250	4.63(0)	8.47(0)	1.17(3)	1.92(−1)	2.15(−1)	1.27(0)	1.19(0)
300	1.41(1)	2.06(1)	1.83(3)	1.78(0)	1.75(0)	6.18(0)	5.87(0)
350	3.92(1)	4.95(1)	2.93(3)	8.83(0)	8.26(0)	2.23(1)	2.13(1)
400	9.27(1)	1.08(2)	4.41(3)	2.96(1)	2.71(1)	6.16(1)	5.93(1)
450	1.90(2)	2.10(2)	6.22(3)	7.66(1)	6.94(1)	1.40(2)	1.35(2)
500	3.47(2)	3.71(2)	8.36(3)	1.65(2)	1.49(2)	2.75(2)	2.65(2)
600	9.01(2)	9.29(2)	1.34(4)	5.28(2)	4.77(2)	7.78(2)	7.53(2)
700	1.85(3)	1.87(3)	1.92(4)	1.23(3)	1.12(3)	1.68(3)	1.62(3)
800	3.26(3)	3.27(3)	2.57(4)	2.36(3)	2.16(3)	3.05(3)	2.92(3)
900	5.15(3)	5.14(3)	3.26(4)	3.96(3)	3.64(3)	4.92(3)	4.66(3)
1000	7.55(3)	7.51(3)	3.99(4)	6.05(3)	5.60(3)	7.29(3)	6.84(3)
1100	1.04(4)	1.04(4)	4.75(4)	8.64(3)	8.03(3)	1.01(4)	9.42(3)
1200	1.38(4)	1.37(4)	5.52(4)	1.17(4)	1.09(4)	1.35(4)	1.24(4)
1250	1.56(4)	1.55(4)	5.92(4)	1.34(4)	1.26(4)	1.54(4)	1.40(4)
Column	2	3	4	5	6	7	8

[a] The units of k are centimeters per molecule per second.

[b] The transition state theory calculations differ in the tunneling correction that has been applied. One calculation ($\kappa=1$) involves no tunneling corrections, the others one-dimensional corrections (κ_1^{VAZC}, κ_1^{CVEZC}, and κ_1^{ECVEZC}) and extended tunneling corrections (κ_2^{VA} and κ_2^{CVE}) as discussed in the text. All calculations in this table except κ_1^{ECVEZC} are from numerical solutions of the Schrödinger equation for the scaled SSMK surface described in Sec. II. The κ_1^{ECVEZC} calculation is based on the Eckart barrier in the usual way. (The numbers in parentheses are powers of 10 by which the preceding numbers must be multiplied.)

While (29) represents an improvement over (26) in taking account that motion along the reaction coordinate is not strictly separable, it is a quantity which is not easily calculated for general reactions and as pointed out in Sec. III.C obviates the need for TST. Therefore, the κ_2 calculation is done only for comparison purposes.

The results of transition state theory calculations using Eqs. (24)–(29) are given in Table IV. In addition the table gives results for the case where the usual Eckart barrier approximation (height and negative force constant of the Eckart barrier equal to those for the CVEZC barrier) is used as a substitute for the numerical integration necessary to use obtain κ_1^{CVEZC} for Eq. (25). This is called the Eckart–CVEZC approximation (ECVEZC).

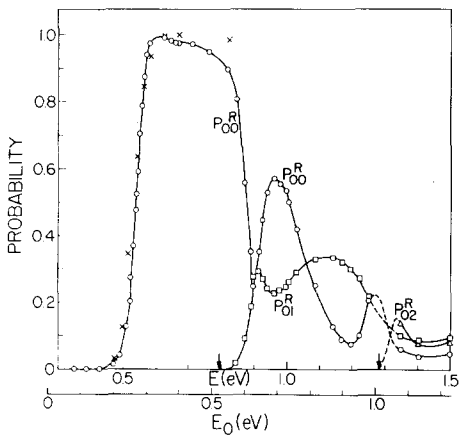

FIG. 3. Probabilities for reactive collisions P_{0n}^R from ground state of reagent to vibrational state n of product ($n=0$, 1, 2) as a function of total energy E and of initial relative kinetic energy E_0. Arrows on E scale are thresholds for formation of vibrationally excited product. Solid curves are results of present calculations, with dashed portions less accurate than rest. The crosses are P_{00}^R obtained by Mortensen and Gucwa,[3] for a different potential energy surface after their E_0 scale is shifted by 0.057 eV (the amount by which their barrier is lower than ours).

V. RESULTS OF EXACT CALCULATIONS

Figures 3–8 show the exact probabilities for reactive and nonreactive collisions of H with H_2 for different

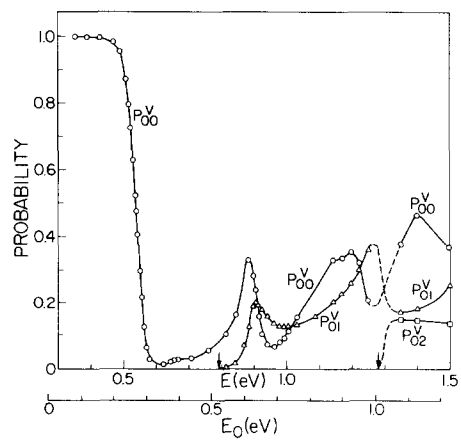

FIG. 4. Probabilities for nonreactive collisions P_{0n}^V, analogous to the reactive ones of Fig. 3.

TABLE V. Probability of reaction at low energy.[a]

Exact		VAZC model		CVEZC model	
E_0 (eV)	$P_{00}{}^R$	E_0 (eV)	$P_{00}{}^R$	E_0 (eV)	$P_{00}{}^R$
0.005	1.85(−7)	0.0461	2.48(−8)	0.0432	2.87(−9)
0.010	3.89(−7)	0.0621	9.00(−8)	0.0492	4.63(−9)
0.020	1.03(−6)	0.0798	2.79(−7)	0.0707	2.12(−8)
0.0432	4.16(−6)	0.0987	1.11(−6)	0.0952	1.04(−7)
0.0809	2.79(−5)	0.1184	3.87(−6)	0.1223	5.34(−7)
0.1174	1.77(−4)	0.1386	1.61(−5)	0.1512	2.85(−6)
0.1572	1.48(−3)	0.1588	5.77(−5)	0.1815	1.53(−5)
0.1980	1.49(−2)	0.1785	2.46(−4)	0.2124	8.03(−5)
0.2170	4.42(−2)	0.1974	7.99(−4)	0.2433	4.00(−4)
0.2361	1.29(−1)	0.2151	2.57(−3)	0.2736	1.84(−3)
		0.2311	9.03(−2)	0.3025	7.48(−3)
		0.2451	2.46(−2)	0.3296	2.61(−2)
		0.2569	5.89(−2)	0.3541	7.45(−2)
		0.2661	1.10(−1)	0.3746	1.68(−1)

[a] Numbers in parentheses are powers of ten by which preceding numbers must be multiplied.

initial and final states of the diatomic molecule, as functions of the total energy E and initial relative kinetic energy E_i. We use the notation $P_{ij}{}^R$ for the probability that a molecule in state i ($i=0$, 1, 2) will react to give a product in state j. Similarly, $P_{ij}{}^V$ denotes the probability that a molecule in state i will collide nonreactively to produce a molecule in state j. These probabilities can be compared to the exact calculations for collinear $H+H_2$ collisions as computed by Mortensen and Gucwa[3] for a different but similar potential energy surface. The barrier height E_b is 0.057 eV lower on their surface; therefore, to make the comparison we add 0.057 eV to each of their relative translational energies. The comparison is shown in Fig. 3. The agreement is as good as could be expected for two different potential energy surfaces; i.e., the small difference in surfaces has apparently not caused any unexpectedly large differences in the probabilities over the energy range they investigated. Diestler[5] has performed more recent calculations for yet another approximate H_3 potential energy surface. His results are qualitatively similar to ours.

It is also interesting to compare our results to some exact calculations for A+BC→AB+C of Tang, Kleinman, and Karplus on a highly simplified surface.[53] They studied a case (their case 4) where all three atoms have equal mass and where the potential energy barrier is $0.833(E_1{}^v-E_0{}^v)$. In the present case the potential energy barrier is $0.814(E_1{}^v-E_0{}^v)$. The comparison is given in Fig. 9 where the probabilities are plotted against $E/E_1{}^v$. This choice of abscissa minimizes differences due to the different vibrational spectra of a Morse oscillator and a particle in a box. The comparison shows that the number of oscillations in the reaction probability curves is the same in both cases; i.e., before the region of the threshold for the second excited vibrational level the $P_{00}{}^R$ curve has two maxima and two minima and the $P_{01}{}^R$ curve has two maxima and one minimum. The qualitative agreement between the two sets of probabilities, when plotted this way, is surprisingly good.

Table V gives the exact reaction probabilities at energies too low to be shown in the figures. The exact results are discussed in Sec. V and the approximate theoretical results in this table are discussed in Sec. VI.E and VI.F.

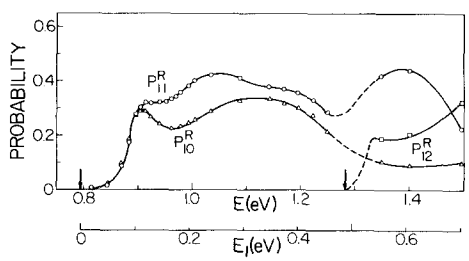

FIG. 5. Probabilities for reactive collisions $P_{1n}{}^R$ analogous to Fig. 3, with initial vibrational quantum number 1. E_1 is initial relative kinetic energy.

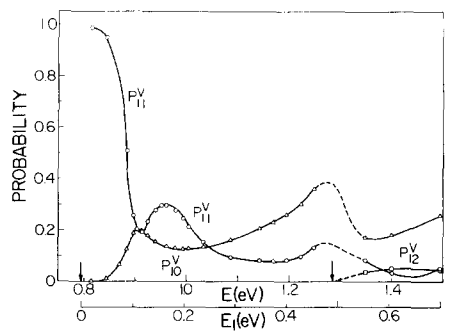

FIG. 6. Probabilities for nonreactive collisions $P_{1n}{}^V$, analogous to Fig. 5.

TABLE VI. Exact rate constants $k_r(n, T)$ for specified vibrational levels and exact thermal rate constants $k_r(T)$.

	$k_r(n, T)$[a]		
T (°K)	$n=0$[b]	$n=1$[c]	$k_r(T)$[a,b]
200	2.07(−1)	···	2.07(−1)
250	1.19(0)	1.5(3)	1.19(0)
275	2.74(0)	2.0(3)	2.74(0)
300	5.87(0)	2.6(3)	5.87(0)
350	2.13(1)	4.0(3)	2.13(1)
400	5.93(1)	5.6(3)	5.93(1)
500	2.65(2)	9.5(3)	2.65(2)
650	1.13(3)	1.6(4)	1.13(3)
800	2.91(3)	2.4(4)	2.92(3)
900	4.63(3)	2.9(4)	4.66(3)
1000	6.77(3)	3.4(4)	6.84(3)
1100	9.30(3)	3.8(4)	9.42(3)
1200	1.22(4)	4.3(4)	1.24(4)
1250	1.37(4)	4.6(4)	1.40(4)

[a] The units of k are centimeters per molecule per second.
[b] Estimated error of about 2%.
[c] Estimated error less than 25% for $T \leq 400$°K and less than 10% for $T > 400$°K. These errors are larger than those for $n=0$ because reaction probabilities were calculated at fewer energies.

Table VI gives the calculated exact one-dimensional rate constant for the ground and first excited vibrational state and also the rate constant computed for a thermal distribution of vibrational states [see Eq. (8)]. As expected from analogy with the three dimensional quasiclassical reaction,[54a] most reactive collisions are shown to involve vibrationally unexcited reagents.

Figure 10 contains an Arrhenius plot of our exact rate constants. Also shown is the Arrhenius fit to the high temperature results

$$k_A(T) = A \exp(-E_a/kT) \qquad (30)$$

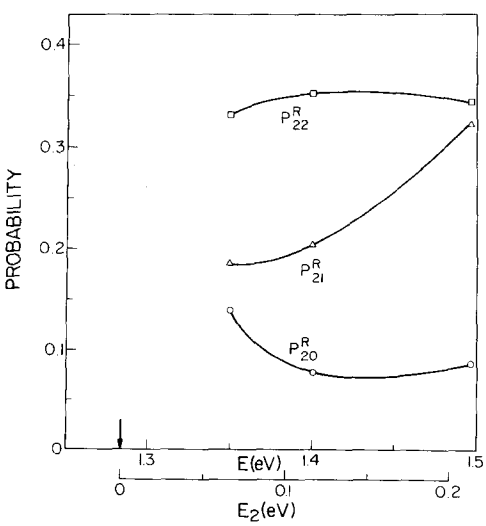

FIG. 7. Probabilities for reactive collisions, $P_{2n}{}^R$, analogous to Fig. 3, with initial vibrational quantum number 2. E_2 is initial relative kinetic energy.

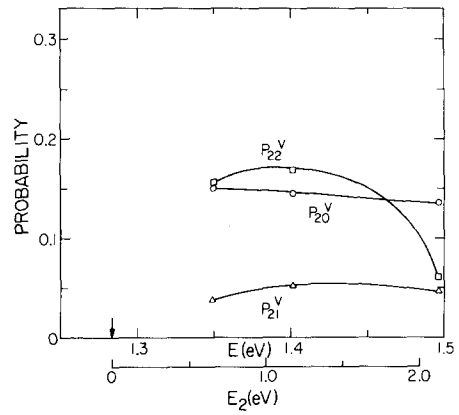

FIG. 8. Probabilities for nonreactive collisions $P_{2n}{}^V$ analogous to Fig. 7.

with $A = 2.20 \times 10^5$ cm/molecule·sec and $E_a = 0.299$ eV. This expression provides a good fit from the highest temperature we considered (1250°K) to about 450°K, where the deviation is 38%. Westenberg and de Haas[17] made an experimental study of H+D₂ and found the Arrhenius plot was linear within their experimental precision (8%) for temperatures above 450°K and nonlinear below that temperature. In the present case, the nonlinearity is 8% at 650°K. Westenberg and de Haas[17] also observed nonlinearity in the Arrhenius plot for D+H₂ but at a lower temperature. Schultz and Le Roy[55] found nonlinearity in their experimental Arrhenius plot for H+H₂ at 320°K and Ridley, Schultz, and LeRoy[56] found nonlinearity in their experimental results for D+H₂ at 300°K. The largest nonlinearity (defined as the ratio of the exact constant to the results predicted by extrapolation of the higher-temperature Arrhenius fit) observed experimentally for the H+H₂ system and its isotopic analogues was 2.6 by Westenberg and de Haas[17] for D+H₂ at 250°K. We find nonlinearities of 2.8 at 300°K and 5.8 at 250°K.

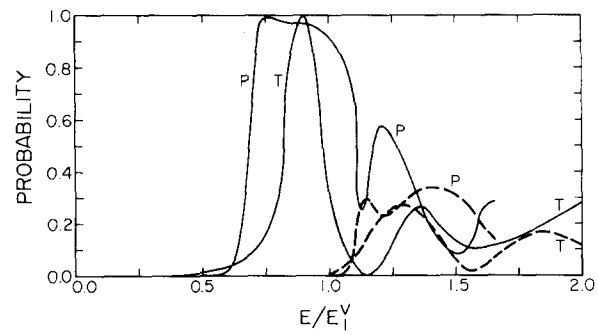

FIG. 9. Comparison of reaction probabilities from present work (P) with model calculations of Tang, Kleinman, and Karplus (T). The solid lines are $P_{00}{}^R$ and the dotted lines are $P_{01}{}^R$. The abscissa is total energy divided by the vibrational energy of the first excited state. The curves in the present case cover the energy range from 0 to the threshold for the second excited vibrational state. In the case considered by Tang *et al.* this threshold occurs at $E/E_{1v} = 2.25$, and in present calculations at 1.62.

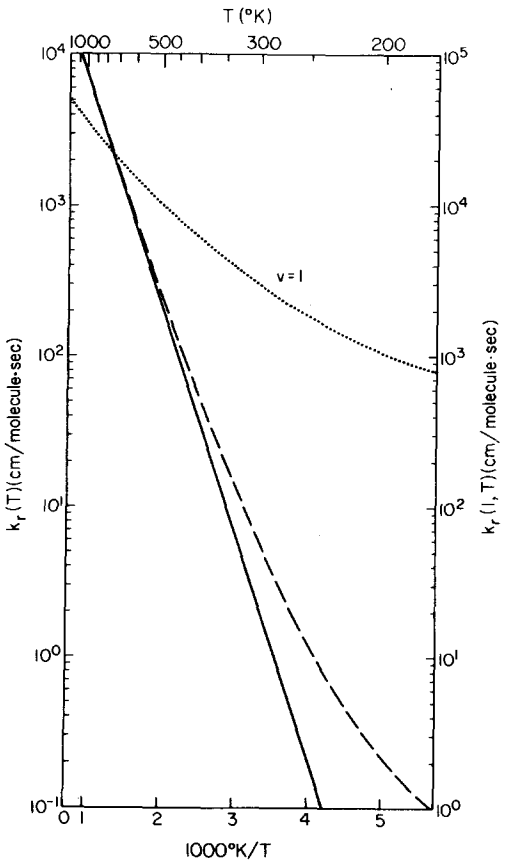

FIG. 10. Accurate rate constant $k_r(T)$ for a Boltzman distribution of vibrational levels (only $v=0$, and $v=1$ are important in this temperature range) vs reciprocal temperature. This result is dashed. It is compared to the Arrhenius fit [Eq. (30)] to the high temperature data. This fit is solid. The ordinate for these two curves is on the left. The dotted curve is $k_r(1, T)$. Its ordinate is on the right.

The usual interpretation of this nonlinearity is that it is due mainly to tunneling. We shall discuss tunneling in Sec. VI.A and in more detail in a subsequent article.

For reactions in three dimensions, a simple model for the reaction probability is that the energy directed along the line of centers of the reagents must exceed a threshold E_t.[57,54] The comparable model for collinear collisions is

$$P_n^{LC}(E_n) = 0 \qquad \text{for } E_n < E_t(n)$$
$$= P_n(\infty) \qquad \text{otherwise,} \tag{31}$$

where E_n is the initial relative kinetic energy when the reagent is in vibrational state n. The reaction probability $P_n(\infty)$ and the threshold energy $E_t(n)$ are constants with respect to E_n. Putting this into (6) yields

$$k_r^{LC}(n, T) = (k/2\pi\mu)^{1/2} P_n(\infty) T^{1/2} \exp(-E_t(n)/kT). \tag{32}$$

If we arbitrarily define the threshold energies to be the energies where the exact probability of reaction curves equal 0.01, we obtain $E_t(0) = 0.198$ eV and $E_t(1) = 0.024$ eV. We define the temperature-dependent effective hard-collision probability of reaction as the quantity $P_n(T)$, which, when replacing $P_n(\infty)$ in (32), would make $k_r^{LC}(n, T) = k_r(n, T)$; i.e.,

$$P_n(T) = (2\pi\mu/kT)^{1/2} \exp(E_t(n)/kT) k_r(n, T).$$

If the line-of-centers model were exact, $P_n(T)$ would be independent of temperature. For the temperature range 200° to 1250°K we find $P_0(T) = 0.11$ to 0.50 and $P_1(T) = 0.06$ to 0.38. Furthermore, for $T = 150$°K, $P_0(T) = 3.05$ and $P_1(T) = 0.06$. The model fails badly at low temperature for the ground vibrational state. While the results are somewhat reasonable, the temperature dependence of the effective hard-collision probabilities are too large for the model to be useful except for qualitative work.

VI. DISCUSSION

A. Low Energy Tunneling

For the relative translational energies less than 0.151 eV and the reactant molecule having zero point vibrational energy, reaction in this system is strictly classically forbidden; i.e., below this energy the total system energy is less than the potential energy of the saddle point and there is no possible classical mechanical trajectory leading from one side to the other. At $E_0 = 0.151$ eV, the reaction probability is 0.0011. Between this energy and 0.043 eV the reaction probability rises exponentially with energy and may be represented very accurately by

$$P(E_0) = \exp[\beta(E_0 - V_0)], \tag{33}$$

where $\beta = 51.1$ eV^{-1} and $V_0 = 0.286$ eV.

The well-known analytical expression[51] for one-dimensional scattering off an untruncated parabolic barrier reduces at low energy to Eq. (33) where the barrier height is $(V_0 - E_0)$ greater than the incident energy and β depends on the curvature of the barrier. The β found empirically in the present case corresponds to an imaginary asymmetric stretch frequency of $922i$ cm^{-1}. This empirical fit of the exact results to a one-dimensional parabolic model leads to an effective parabolic barrier height close to the 0.277 eV VAZC barrier and an effective parabolic asymmetric stretch frequency close to the $1550i$ cm^{-1} frequency found by normal mode analysis[29] of the classical potential energy surface.

As E_0 approaches 0, so does $P(E_0)$. However, Eq. (33) furnishes $P(0) = 4.5 \times 10^{-7}$. This small deviation between the exact results and the fit of Eq. (33) in the energy range 0 to 0.04 eV is sufficiently large, nevertheless, to produce substantial errors in the thermal rate constants below 250°K if Eq. (33) rather than the exact results in this energy range were used in Eqs. (6)–(8). A more accurate fit at very low ener-

gies is given by the expression

$$P(E_0)=e^{-\beta V_0}[\exp(\beta E_0)-1]. \quad (34)$$

This equation satisfies the condition $P(0)=0$. In the energy range 0.005 to 0.081 eV the values $\beta=45.91$ and $V_0=0.309$ eV make Eq. (34) agree with the exact values of $P(E_0)$ within 4% or better.

Discussions of quantum mechanical tunneling often are confused by not having a good definition of tunneling. The nonzero reaction probabilities we find at $E_0<0.151$ eV are quantum mechanical tunneling even in the strictest sense of the word as discussed above. However, the transmission probabilities at energies even 0.1 eV higher than that could be called tunneling, depending on the definition used. A particularly rigorous definition would be based on the probability current density vector and the associated stream lines. The fraction of the flux of this current density into the separated product region of configuration space that is associated with stream lines that have penetrated into classically forbidden regions (i.e., regions of negative total kinetic energy) is a very general and model-independent definition of a tunneling coefficient. Calculations using this definition are being carried out with some of the present wavefunctions. In a subsequent publication we will use this definition and report the corresponding tunneling coefficients. Other definitions are based on models for the distribution of energy between translation and vibration. Using the VAZC model, for which the height of the corresponding barrier is $E_0^{VAZC}=0.2759$ eV [see Eq. (12), and Table II], for this distribution, even at $E_0=0.25$ eV, say, there is a negative translational energy along the reaction coordinate at the barrier and in this model the reaction proceeds entirely by tunneling. The VAZC model is discussed in Secs. III.B and VI.F.

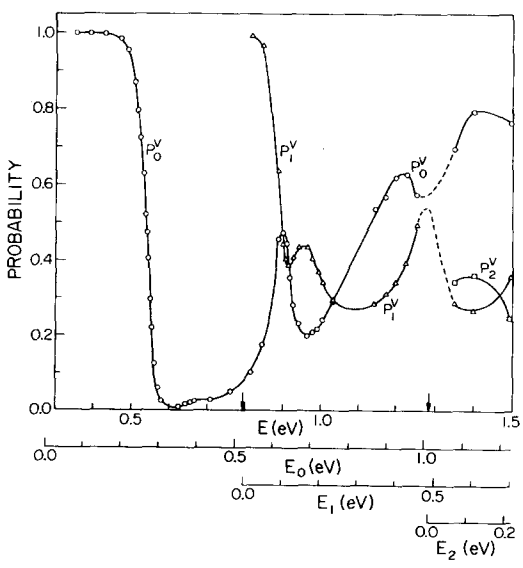

FIG. 11. Total probabilities for nonreactive collisions $P_i^V(i=0, 1, 2)$ as a function of total energy E and relative initial kinetic energy E_i for ground state ($i=0$), first excited state ($i=1$) and second excited state ($i=2$) reagents.

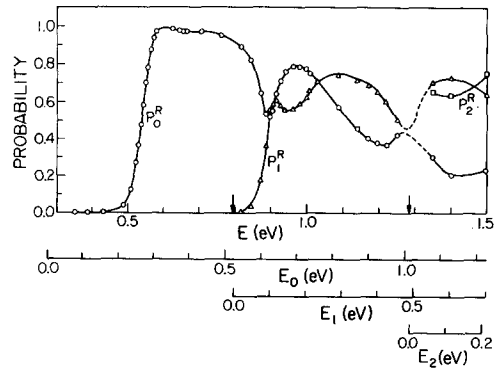

FIG. 12. Total reaction probabilities $P_i^R(i=0, 1, 2)$ as a function of total energy E and relative initial kinetic energy E_i for ground state ($i=0$), first excited state ($i=1$) and second excited state ($i=2$) reagents.

B. Energy Region above Excitation Threshold

As the relative kinetic energy for ground state reagents exceeds the threshold energy for inelastic excitation, the elastic probability P_{00}^V goes through three maxima as shown in Fig. 4. The first occurs slightly above the first excitation threshold and the third above the second excitation threshold. This is an interesting phenomenon, since it suggests that as more competing channels open up, the probability associated to the elastic channel increases. This behaviour may be fortuitous, but it deserves further investigation concerning generality and mechanism. The total nonreactive probability P_0^V exhibits a similar energy dependence, as shown in Fig. 11.

The threshold for production of H_2 molecules in their first vibrationally excited state is 0.79 eV. From that energy to 0.89 eV, vibrationally excited reagents have 0.79 eV vibrational energy and 0.0 to 0.1 eV translational energy, while ground-vibrational-state reagents have 0.27 eV vibrational energy and 0.52–0.62 eV translational energy. Figure 12 shows that for this energy region, the probability of reaction is much greater for ground state reagents. This illustrates that it is not necessary merely to have enough energy to react, but that the energy must be dynamically available to overcome the barrier. Apparently the dynamics of the system require more of the vibrational energy to remain tied up as motion transverse to the curved reaction path in the case where the reagent initially has a greater fraction of energy in this transverse mode. This requirement is an indication of the difficulty of changing the local vibrational energy in this energy region.

The classical and quasiclassical trajectory calculations on the collinear and three-dimensional H+H_2 reaction, by Wall, Hiller, Mazur, Porter, Karplus, and Sharma,[54] did not include a study of vibrationally ex-

TABLE VII. Average reactive and inelastic collision probabilities for different initial vibrational states at energies above second threshold.

Initial state i	$P_i^{\Delta v}$ [a]	P_i^{R} [b]
0	0.56	0.28
1	0.58	0.69
2	0.52	0.68
Average[c]	0.55	0.55
Statistical[d]	0.67	0.50

[a] Probability for change of vibrational state (reactive plus nonreactive) averaged over energy, for energies above second excitation threshold.
[b] Probability of reaction, averaged as above.
[c] Average over initial states i.
[d] Prediction of statistical theory of Lin and Light.[21]

cited molecules. However, a similar effect was noticed in comparing the threshold energy for reaction of reagent having zero point vibrational energy with that of reagent having *no* initial vibrational energy.

At energies more than 0.1 eV above the vibrational excitation threshold, the reaction probabilities of systems with the same total energy but different initial vibrational energies become comparable (see Fig. 12). According to the statistical theory of collinear reactions discussed in the next section, the probability of reaction is independent of initial vibrational state for systems with the same total energy. The next section thus provides a more quantitative discussion of this energy region.

C. Comparison with Statistical Theory

The exact results are in qualitative agreement with the statistical theory predictions that between the first and second excitation thresholds the total probability of reaction (into ground plus excited product) is 0.5 and the total probability of a change of vibrational state (for reactive plus nonreactive collisions) is 0.5. To obtain a more quantitative comparison we must choose the theory's parameters. Since there is no good *a priori* criterion for picking E_A^0 and λ_v [see Eq. (20)], we treat them as adjustable empirical parameters of the theory. Setting $E_A(0)=0.2489$ eV (the translational energy where the probability of reaction is 0.25) and $E_A(1)=0.0820$ eV (the translational energy where the probability of reaction of vibrationally excited molecules is 0.25) gives $E_A^0=0.336$ eV and $\lambda_v=0.32$, a reasonable pair of values. With these parameters, the range of total energies for which the theory predicts the total probability of a change of vibrational state to be 0.5 and the total probability of reaction to be 0.5 is 0.876 to 1.283 eV (the theory actually predicts the probability of reaction to be 0.5 for *all* total energies above 0.522 eV). In this energy range the exact results show an average (over initial energy) probability of change of vibrational state of 0.48 (irrespective of initial vibrational level) and an average probability of reaction of 0.56 for initial vibrational level $v=0$ and 0.63 for initial vibrational level $v=1$. Thus after fitting E_A^0 and λ_v empirically there is good quantitative agreement with the predictions of the statistical theory *on the average* and the exact results tend to oscillate around their statistical values. The amplitude of the oscillations is about 30%.

Lin and Light[21] point out that some information about λ_v could be obtained by comparing reaction thresholds in classical and quasiclassical trajectory calculations; in particular, the collinear trajectories of Karplus, Porter, and Sharma[54b] yield $\lambda_v=0.62$ when analyzed this way. No reasonable agreement can be obtained with this value of λ_v or with $\lambda_v=1.0$ as assumed for the treatment of experimental data by Lin and Light.[21]

The parameters used above predict $E_A(2)=0.0$. We have not made a detailed study of the second threshold but our limited results do indicate the effective $E_A(2)$ must be very small, surely less than 0.03 eV and probably less. Thus there is agreement of the theory and the exact results in that there is no significantly delayed onset of reaction at the second threshold. For the parameters above, it turns out that the statistical theory predicts that for total energies in the range 1.283 to 1.74 eV the probability of change of vibrational state (for reactive plus nonreactive collisions) is 0.67 and the probability of reaction is 0.5 (both irrespective of initial vibrational level). Our limited results (5 energies in the range 1.323 to 1.497 eV) are summarized in Table VII. There is fair agreement in this case also, but more definite conclusions are precluded by the small sample of exact results.

The general conclusion is that the statistical approximation is correct in spirit for this reaction at total system energies greater than about 0.86 eV. The statistical theory is even, in some cases, semiquantitatively accurate; however, the more important conclusion is that it is entirely correct in its general prediction that there is appreciable probability for all processes which are energetically allowed and that *all* these processes occur with about equal probability.

For two reasons, it should perhaps not be surprising that the statistical theory works well for this reaction. First, the potential surface is a simple repulsive barrier. This should favor impulsive reaction models. Second, collinear collisions should be harder and more impulsive than sideways collisions. It is possible to justify[58–60] the statistical theory using the sudden approximation, which is an impulsive model. This is probably the reason for the success of the statistical theory at high energies (total system energy greater than about 0.86 eV) in the present case.

D. Oscillations in Cross Sections

In the region above the vibrational excitation threshold where the statistical theory appears useful, there are important oscillations in every reactive and nonreactive probability vs energy curve. In an early study of the quantum dynamics of the H+H$_2$ reaction, Micha[61] found fairly rapid oscillations in the probability curves at energies below the vibrational excitation threshold. This calculation was made using an approximate distorted wave method. Subsequently, Karplus and Tang[28] did further calculations using this general type of approach but eliminating many of the simplifying assumptions made in the earlier treatment. In the calculations of Karplus and Tang the oscillations below the vibrational excitation threshold do not appear. This indicates the oscillations in Micha's probability curves were artifacts of his simplifying approximations. These calculations were not extended to energies above the excitation threshold since the distorted wave method becomes inaccurate[62] when the transition probability becomes fairly large. In our exact calculations we find no oscillations below the excitation threshold.

The oscillations we observe in the probability curves above the excitation threshold are similar to those often observed in quantum calculations of vibrational excitation in nonreactive collisions. (See, e.g., Refs. 63–66). These are most easily explained using Miller's and Marcus's semiclassical theories.[67,68] According to these theories, the oscillations are due to interfering amplitudes for different semiclassical paths between reagents and products with the correct quantized energy levels.[69,70] The oscillations observed in both the nonreactive and the reactive probability curves in this work should be explainable in terms of this semiclassical theory, although calculations for this reactive class have not yet been reported. Such calculations are also being performed in our laboratory.

E. Comparison with Conservation of Vibrational Energy Theory

The two-mathematical-dimensional problem of collinear collisions can be reduced approximately to a one-dimensional problem by making an assumption which separates out one of the degrees of freedom. If we assume the vibrational energy is conserved throughout the reaction we reduce the reactive scattering problem to transmission across a barrier which is the classical potential energy along the reaction path. This one-dimensional problem may be solved classically or quantum mechanically. Comparison of these two CVEZC treatments with the exact results for probability of reaction of reactants in the ground vibrational state is given in Fig. 13. The model is not very accurate; it predicts a high threshold energy because it uses the full classical barrier height which ignores

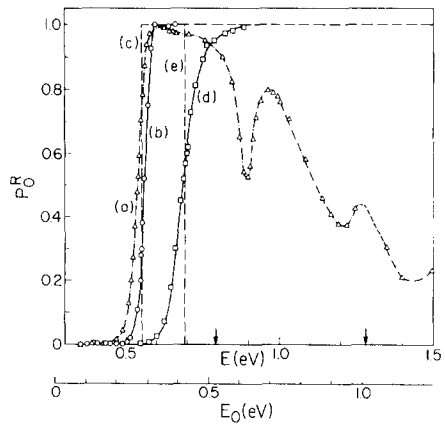

FIG. 13. Accurate and approximate reaction probabilities P_0^R for ground state reagent as a function of total energy E and of initial relative kinetic energy E_0. Arrows on E scale are thresholds for formation of vibrationally excited product. Curve (a) is the result of the exact calculations. Curves (b) and (c) are VAZC results for the quantum and classical versions of this model, respectively. Curves (d) and (e) are the corresponding CVEZC results.

contributions from the zero point energy of the reagent. In addition, the variation of the CVEZC quantum reaction probability with energy is far too slow because of excessive tunneling through the thin CVE barrier and excessive nonclassical reflection.

F. Comparison with Vibrationally Adiabatic Theory

Another way to separate the degrees of freedom from one another is to assume vibrational adiabaticity (VA) as in the vibrationally adiabatic zero-curvature model (VAZC), discussed in Sec. IV.B. The reaction probabilities $T_1(E_0, 0)$ discussed there are shown in Fig. 13. This model is in much better agreement than the CVEZC one with the exact results. However, it too fails at very low energies. Table V shows that when the exact probability of reaction is less than 0.1, neither of the methods we use to separate the degree of freedom gives accurate results.

For an untruncated parabolic one-dimensional barrier, the probability of reflection is 0.50 for an energy exactly equal to the barrier height.[71] For a more general barrier, this is only approximately true. Because of the broad plateau on the lowest VAZC barrier for the collinear H+H$_2$ reaction, the VAZC probability of reaction is 0.29 for an energy equal to the barrier height and 0.50 for an energy 0.010 eV above the barrier height. The correct reaction probability at these two energies is 0.62 and 0.76 respectively.

There are two reasons why the VAZC quantum mechanical calculation does not agree perfectly with the exact results: (1) the VA separation of the transverse vibrations is only an approximation, i.e., the reaction is not perfectly vibrationally adiabatic; (2) the neglect of curvilinear effects in treating the VAZC model is a further approximation. The second reason

involves two important effects: (a) a centrifugal effect causing the actual reaction path to lie off the minimum energy reaction path; (b) the approximation of calculating transmission over a barrier in one curvilinear dimension by simply straightening out the path. Because of approximation (2) the VAZC calculation is not a direct test of vibrational adiabaticity. It is actually a test of a model which both neglects curvilinear effects and assumes vibrational adiabaticity. We will consider a test of vibrational adiabaticity itself in a future article.

The breakdown of approximation (1) may semiclassically be described as leading in part to reacting particle trajectories "cutting the corner" (i.e., crossing the $R_{AB}=R_{BC}$ line with R_{AB} larger than its saddle point value) or otherwise crossing the $R_{AB}=R_{BC}$ line in a nonadiabatic symmetric-stretch vibrational state. However, the centrifugal effect usually (an important exception is discussed below) tends to make the reaction coordinate lie on the convex side of the minimum energy path.[47] For this reason it has been called the bobsled effect.[24] Thus, it is possible that approximations (1) and (2a) may cancel to some extent. Only a more direct test of vibrational adiabaticity without further assumptions will determine the full extent of such cancellation. The fact that the exact reaction probability for a translational energy equal to the VAZC barrier height is 0.65 rather than the 0.29 predicted by the VAZC model suggests that one must be cautious in stressing the VAZC requirement that energy of the system at the transition state be tied up adiabatically as zero point energy of the transverse symmetric stretching vibration. In addition, if it turns out upon evaluation of the tunneling coefficient via probability current densities (as mentioned in Sec. VI.A) that reaction at energies at and just below the VAZC barrier height proceeds mainly via classically allowed region (i.e., regions of positive total kinetic energy), the validity of the VAZC approximation will have to be further reevaluated since according to it the reaction at these energies proceeds via tunneling. Nevertheless, it is important to emphasize the success of the VA model used here as a practical tool for reproducing important aspects of the full calculation by means of a much simpler one. Its success also indicates it could be useful and valid for predicting qualitative trends in similar processes.

Wyatt[46] has quantitatively studied curvilinear effects within the VA model for a near-linear $H+H_2$ collision in a plane. His calculations indicate that the VAZC model for that case predicts appreciable reaction at energies about 0.02–0.04 eV lower than models assuming vibrational adiabaticity but not assuming zero curvature. If the effects of curvature are in the same direction for the case studied here then the assumptions (1) and (2) do indeed lead to partially compensating errors.

Table V compares the exact reaction probabilities at very low energies with the predictions of the CVEZC and VAZC models. The VAZC model is closer than the CVEZC one to the exact results but both models fail badly in this energy region where the reaction probability is very small. This means that the full two-dimensional treatment is necessary to adequately describe this tunneling region; curvilinear effects cannot be ignored. Marcus[24,26] has pointed out that for the energy range with translational energies below the VA barrier the centrifugal effect is negative and causes the reaction coordinate to lie on the concave side of the minimum energy path. Thus the reaction most probably cuts the corner and the quantum mechanical interaction of the translational and vibrational modes is very important. McCullough and Wyatt's studies of the collinear $H+H_2$ reaction[7] by time-dependent quantum mechanics have shown that an important reaction route for low energy particles is a diagonal cut across the center. This is most likely the same phenomenon we observe here.

The interpretation that a cut across the barrier at large R_{AB}, R_{BC} becomes a more favorable tunneling path at very low energies than proceeding along the minimum energy reaction path is consistent with the exact results being *larger* than the one-dimensional model results at low energy. Then the VAZC model results show that the reaction probability would be about two orders of magnitude smaller at low energies if the system were forced to proceed along the minimum energy reaction path. Calculation of the probability current densities and streamlines from our scattering wave functions should give useful information on these points. Such calculations are in progress.

The failure of the one-dimensional models at low energies has important implications for the usual one-dimensional tunneling calculations.[13–16,18–20,44,45] It means that these one-dimensional theories cannot be used at low temperature where the tunneling correction is very sensitive to the low-energy transmission probabilities. This defect of the one-dimensional theories will be discussed in the next subsection (VI.G).

At translational energies of 0.08–0.22 eV, the de Broglie wavelength for the relative motion of $H+H_2$ is 1.2 to 1.6 Å. This is large compared to the range of internuclear distances near the saddle point over which the normal-mode coordinate separation is valid.[2,15] Thus, at low energies the separation of vibration and translation is not expected to be a good approximation. This is why a quantum mechanical treatment in two mathematical dimensions is necessary.

At energies above the threshold we find appreciable probabilities for the change of vibrational state. These probabilities violate the vibrationally adiabatic approximation. Thus the VA approximation appears to be bad for total energies above about 0.85 eV. It is interesting, however, that in the region above the first threshold, $P_{00}{}^{R}>P_{01}{}^{R}$ and $P_{11}{}^{R}>P_{10}{}^{R}$, i.e., the reaction probability is a little greater for the reactive channel

in which the vibrational quantum number is conserved. This is a small remnant of the success of the VA theory at lower energies.

G. Comparison with Transition State Theory

The comparison of the accurate results with transition state theory including one-dimensional tunneling corrections has been discussed briefly in a preliminary communication.[72] Further comparison is made in Table IV and Figs. 14 and 15.

The transition state theory without tunneling is inaccurate by 11% at 1000°K. This means it is a good working hypothesis for the interpretation of experimental data to assume such a transition state theory calculation is accurate at temperatures around 1000°K. At 1250°K, the error is 2%. We have not tested transition state theory at temperatures higher than this. At 750°K the error is 21% and in the 444° to 300°K range for which Schulz and LeRoy studied H+H₂ experimentally, the theory is 43 to 70% low.

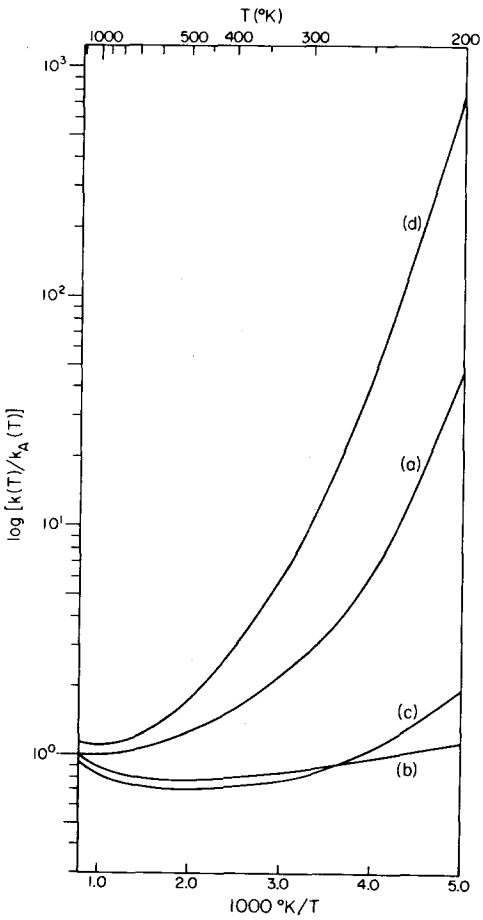

FIG. 14. Accurate rate constant and three transition state theory rate constants for the collinear H+H₂ reaction as functions of reciprocal temperature. Each rate constant is divided by the Arrhenius fit $k_A(T)$ so that the plot indicates the deviations of the exact and the three approximate Arrhenius plots from nonlinearity. Curve (a) is the accurate rate constant and curve (b) is transition state theory rate constant without tunneling. The other curves are transition state theory calculations including tunneling along the one-dimensional minimum energy path as calculated by (c), the VAZC approximation, and (d) the ECVEZC approximation. See Secs. IV.C and VI.G of text.

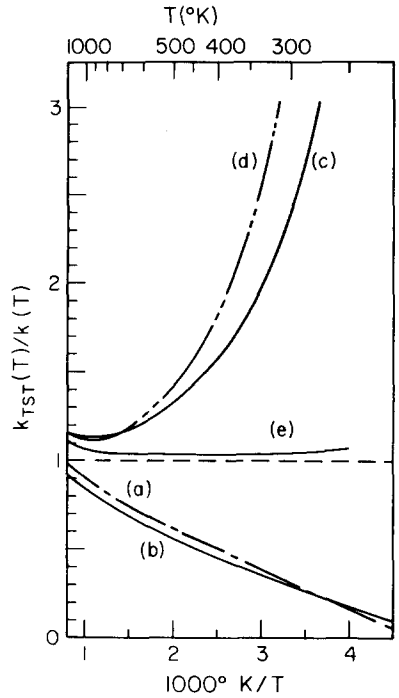

FIG. 15. The ratios of five TST rate constants to the accurate one, as functions of reciprocal temperature. Different one-mathematical dimensional (1-MD) transmission coefficient corrections are used: (a) classical motion for a Cartesian reaction coordinate, (b) quantum vibrationally adiabatic zero curvature (VAZC) model, (c) quantum conservation of vibrational energy zero curvature (CVEZC) model, (d) analogous to (c) with Eckart fit to the height and the curvature at the top of the CVEZC barrier. In Curve (e) the 2-MD transmission coefficient of Eq. (14) with $E_0^b = E_0^{VAZC}$ is employed. The horizontal dashed line would represent the results of an exact theory.

According to the vibrational adiabatic derivation of transition state theory,[25,27,73] the potential energy responsible for motion along the reaction coordinate is the vibrationally adiabatic potential. Hence, formally, if a one-mathematical-dimensional (1-MD) tunneling correction is made, it should be for such a potential barrier.[45] Table IV and Figs. 14 and 15 show, however, that the numerically calculated 1-MD VAZC tunneling correction is much too small at low temperature and is in the right direction only at temperatures less than 290°K. Fig. 13 shows, however, that this tunneling correction improves the temperature dependence of TST below about 500°K [i.e., in this range the slope of Curve (*c*) is closer than the slope of Curve (*b*) to that of Curve (*a*)]. The low-temperature results are sensitive to the low-energy reaction probabilities which we have seen (Sec. VI.F) are too large to be explained by a treatment which separates out the reaction coordinate. The two-mathematical-dimensional (2-MD) VA tunneling correction leads to transition state theory rate constants (next to last column of Table IV) in

TABLE VIII. Ratio of accurate to transition state theory rate constants.[a]

T (°K)	Karplus *et al.*[b,c]	Present work[c]	Mortensen[c,d]
200		29.79	
300	6.13	3.30	25.08
400	3.20	2.00	8.26
500	2.25	1.61	4.72
600	1.81	1.42	3.38
700	1.57	1.31	2.72
800	1.41	1.23	2.33
900	1.29	1.17	2.07
1000	1.20	1.12	1.90
1100		1.08	
1200		1.04	
1250		1.02	

[a] This ratio is the quantity $\kappa_e(T)$ defined by Eq. (15).

[b] These are the results of Karplus, Porter, and Sharma (Ref. 54) for the quasiclassical three-dimensional reaction.

[c] Three different but very similar potential energy surfaces were used for the calculations in this table.

[d] These are the results (Ref. 2) for the quantum mechanical 3-MD reaction with the approximation of collinear collisions on a potential energy surface incorporating a correction to take approximate account of bending from the collinear configuration.

much better agreement with experiment than the one-dimensional tunneling correction. It is possible that an appropriate 2-MD treatment could be used for the noncollinear collision as an improvement over the VAZC theory. However, it is basically inconsistent with the assumption of reaction coordinate separability in transition state theory.

The CVEZC and ECVEZC one- and two-dimensional tunneling calculations are included for completeness. The CVEZC tunneling correction has been discussed in an earlier article[45] where we showed that it is inconsistent with transition state theory so that we cannot give these results a dynamical interpretation. Table IV shows that in the present case there are large deviations between it and either the transition state theory calculations with VAZC tunneling or the accurate results. Nevertheless the transition state theory calculations with 1-MD CVEZC and ECVEZC tunneling corrections show large nonlinearity on an Arrhenius plot (see Fig. 14), and in this regard they resemble the accurate results. Since these calculations are based on conservation of energy of the transverse vibration as the system proceeds along the reaction path and since this is known (Fig. 13) to be a poor dynamical approximation, we cannot learn much about the reaction from such calculations (which are very common) even if we ignore the formal difficulties referred to in the second sentence of this paragraph. At 200°K, the ECVEZC rate constant is 23 times the correct one, and the CVEZC calculation, which contains one less approximation, is still 10 times too large.

These transition state theory calculations for a case where accurate rate constants are known and the potential energy surface is known provide an important test of the theory. Previous tests (see Refs. 74 and 75 for recent summaries) were complicated by lack of knowledge of the real potential surface. The conclusion of our work is that transition state theory, although qualitatively correct, is not a good enough model to explain the accurate rate constants quantitatively. Thus the theory cannot be used to obtain unknown potential surfaces except approximately.

Karplus, Porter, and Sharma[54] made a test of transition state theory against their quasiclassical trajectory calculations for the three-dimensional $H+H_2$ reaction. Their results are compared to ours in Table VIII. They find larger transmission coefficients than are found in the present work. One reason for this is the lack of quantization of vibrational modes (other than in the initial conditions) in the quasiclassical calculation. This releases energy from the symmetric stretch vibrational mode of the transition state into the reaction coordinate and thus increases the reaction probability. Since the physical mechanisms behind their and our transmission coefficients are so different, it is not surprising that they quantitatively show little agreement.

H. Comparison with Mortensen's Calculations for Linear Collisions with Bending Corrections

Mortensen,[2] in a continuation of the now classic work of Mortensen and Pitzer,[1] calculated $\kappa_e(T)$ for quantum mechanical collinear collisions with bending corrections to make the results be an approximation to the experimental reaction. His results as given in Table VII are larger than the present ones. This is easily understood in terms of the nature of the bending corrections to the potential energy surface. These corrections make his barrier thinner than ours; thus there is more tunneling in his case.

Another important observation by Mortensen[2] was that the curve representing the accurate probability of reaction rises steeply at an energy about 0.040 eV less than would be expected on the basis of the VAZC model (see Fig. 8 of Ref. 2). We obtain a qualitatively similar result (see Fig. 3 of this article). However, we find a downward shift in this energy of only 0.010 eV. Mortensen's interpretation was that the effective zero point energy of the transition state symmetric stretch cannot be calculated by a normal mode analysis of the transition state, i.e., by the VAZC model. The comparison of the two sets of results shows that the VAZC model is better for the symmetric stretching mode in the absence of the bending modes (our collisions only involve the symmetric stretching mode) than in their presence. A small shift (of the size we observed) is not unexpected on the basis of the nonseparability of vibration and translation as discussed in Sec. VI.F.

VII. SUMMARY

Reaction probabilities and rate constants have been obtained for the collinear $H+H_2$ reaction on a realistic potential energy surface which are accurate to within 2% or better. These results can be used to test approximate models of chemical reactions. The range of relative translational energies considered was 0.005–1.22 eV.

We find that tunneling is important at low energies. We find effective translational energy thresholds of about 0.25 and 0.08 eV for reaction of $v=0$, and $v=1$ molecules, respectively, but hardly any (<0.03 eV) threshold for reactions of $v=2$ molecules. This indicates the efficiency with which energy can be used to overcome the barrier. At energies above the threshold for vibrational excitation quantum mechanical oscillations in the reactive and nonreactive probability curves (as functions of energy) are very important and are attributed to interference effects.

Our reaction probabilities are compared with the vibrationally adiabatic theory of reactions and with the statistical phase space theory. They agree well with the former for total energy (in the center-of-mass system) in the range 0.49–0.85 eV and with the latter for total energies greater than these. At energies below about 0.49 eV no simple theory seems to predict the accurate results properly.

Our rate constants are compared with unit transmission coefficient transition state theory. They disagree by about the same factor as found in previous tests of this theory by Karplus, Porter, and Sharma and by Mortensen. Because the vibrationally adiabatic assumption fails to predict reaction probabilities accurately at very low energy, transition state theory calculations using a transmission coefficient calculated by the vibrationally adiabatic model do not agree well with the accurate results in the low temperature region where quantum mechanical effects on the transmission coefficient are important. The calculations also indicate that much more tunneling is present than was observed in previous experiments when the three-dimensional $H+H_2$ reaction is studied at lower temperatures. Other details of our results are also discussed.

Our calculations provide an example of the exact quantum dynamics for a realistic model system. However, in many detailed respects the results are indicative only of the dynamics in similar systems, i.e., light atoms scattering on a potential surface with a simple symmetric barrier. The methods used in this study are general, however, and further applications to other potential surfaces and heavier atoms are necessary to provide more understanding of the quantum dynamics of chemical reactions.

In the present article we have concentrated on the reaction probabilities and rate constants. The former are the results of single collisions and the latter are averages over the results of many collisions. To gain further insight we feel it is important to study the wavefunction and the corresponding probability current densities in the interaction region where all internuclear distances are small (in a time-dependent calculation this could correspond to studying the results before even a single collision was finished). In most quantum mechanical calculations carried out so far the emphasis has been on the reaction probabilities alone. We are continuing the present calculation[76] by studying the wavefunctions and current densities and these results will be reported subsequently.

ACKNOWLEDGMENTS

The authors are grateful to Dr. Dennis J. Diestler, Dr. Nicholas W. Winter, Dr. Merle E. Riley, and Dr. L. M. Delves for valuable discussions or correspondence concerning the method used to solve the Schrödinger equation. We are grateful to Dr. John T. Adams, Joel M. Bowman, and Baruch Kuppermann for performing some of the computer calculations. We would also like to thank Dr. Winter, Dr. Christopher A. Parr, F. P. Roullard III, and the Caltech Booth Computing Center consulting staff (under the direction of Kiku Matsumoto) for help with difficulties involved in the calculations reported here and elsewhere and for useful computer subprograms. We are grateful to Professor William H. Miller for discussions of the results. The work reported here was finished and this article was written while one of the authors (D. G. T.) was in the Department of Chemistry of the University of Minnesota. We are grateful to the University of Minnesota Computing Center for a computing time subsidy.

APPENDIX A

R Matrix Analysis

In this appendix we use the notation of Ref. 32 wherever possible. The elements of the velocity matrix $\mathbf{V}$ are defined by

$$V_{ij}=v_i\delta_{ij}, \tag{A1}$$

where v_i is the relative velocity in channel i, i.e.,

$$v_i=\hbar k_i/\mu_i, \tag{A2}$$

where μ_i is the reduced mass of relative motion of the atom and molecule in channel i. There are N open channels and $T-N$ closed channels corresponding to A+BC and N' open channels and $T'-N'$ closed channels corresponding to AB+C. Let $N''=N+N'$ and $T''=T+T'$ so that V is of dimensions $N''\times N''$. We obtain T'' linearly independent numerical solutions χ_i of the Schrödinger equation. The matrices $\tilde{\mathbf{A}}$ (of dimensions $N''\times T''$), $\mathbf{A}(T''\times T'')$, and $\mathbf{I}'(T''\times N)$ are

defined in Ref. 32. Let $\mathbf{I}''(T''\times N')$ be defined as

$$\mathbf{I}''=\begin{pmatrix}\mathbf{0}_1\\ \mathbf{I}\\ \mathbf{0}_2\end{pmatrix}, \tag{A3}$$

where $\mathbf{0}_1$ and $\mathbf{0}_2$ are null matrices of dimensions $(T\times N')$ and $([T'-N']\times N')$, respectively, and $\mathbf{I}$ is an identity matrix of order N', and let $\mathbf{I}^{\mathrm{D}}(T''\times N'')$ be

$$\mathbf{I}^{\mathrm{D}}=(\mathbf{I}'\mathbf{I}''). \tag{A4}$$

The analysis procedure used by Diestler and McKoy is equivalent to the scattering matrix analysis where the probability of going from initial state i to final state j is

$$P_{ij}=|S_{ji}|^2, \tag{A5}$$

where

$$\mathbf{S}=-\mathbf{V}^{1/2}\bar{\mathbf{A}}\mathbf{A}^{-1}\mathbf{I}^{\mathrm{D}}\mathbf{V}^{-1/2}. \tag{A6}$$

The reactance matrix analysis proceeds analogously except that the asymptotic form of the χ's is expressed in the notation of Ref. 32 as

$$\chi_j=\sum_{l=1}^{N}\{D_l^{(j)}\sin[k_l(\alpha x_{12}+x_{23})]+\bar{D}_l^{(j)}\cos[k_l(\alpha x_{12}+x_{23})]\}\phi_l(x_{12})$$
$$+\sum_{l>N}\{B_l^{(j)}\exp[-k_l(\alpha x_{12}+x_{23})]+\bar{B}_l^{(j)}\exp[k_l(\alpha x_{12}+x_{23})]\}\phi_l(x_{12}),\qquad x_{23}\geq x_{23}^{(0)},$$

$$\chi_j=\sum_{l=1}^{N'}\{\delta_l^{(j)}\sin[k_l'(\alpha x_{23}+x_{12})]+\bar{\delta}_l^{(j)}\cos[k_l'(\alpha x_{23}+x_{12})]\}\bar{\phi}_l(x_{23})$$
$$+\sum_{l>N'}\{\beta_l^{(j)}\exp[-k_l'(\beta x_{23}+x_{12})]+\bar{\beta}_l^{(j)}\exp[k_l'(\beta x_{23}+x_{12})]\}\bar{\phi}_l(x_{23}),\qquad x_{12}\geq x_{12}^{(0)} \tag{A7}$$

TABLE IX. Reactance, scattering, and probability matrices for $E=0.9678$ eV.[a,b]

Extrapolated reactance matrix[c]

1.852	−2.305	1.613	−2.422
−2.281	2.003	−2.399	2.422
1.613	−2.422	1.852	−2.305
−2.399	2.422	−2.281	2.003

Extrapolated scattering matrix[c]

0.2686−0.0034i	0.3234−0.1773i	−0.6025−0.4572i	0.2950−0.3817i
0.3274−0.1790i	0.1673−0.5342i	0.2938−0.3926i	−0.5765+0.1317i
−0.6025−0.4572i	0.2950−0.3817i	0.2686−0.0034i	0.3234−0.1773i
0.2938−0.3926i	−0.5765+0.1317i	0.3274−0.1790i	0.1673−0.5342i

Probability matrix from preceeding extrapolated scattering matrix[c,d]

0.0722	0.1392	0.5720	0.2405	1.0239[e]
0.1360	0.3134	0.2327	0.3497	1.0318[e]
0.5720	0.2405	0.0722	0.1392	1.0239[e]
0.2327	0.3497	0.1360	0.3134	1.0318[e]
1.0129[f]	1.0428[f]	1.0129[f]	1.0428[f]	

Extrapolated probability matrix from symmetrized reactance matrices[d,g]

0.0710	0.1328	0.5661	0.2301	1.0000[e]
0.1328	0.2928	0.2301	0.3444	1.0000[e]
0.5661	0.2301	0.0710	0.1328	1.0000[e]
0.2301	0.3444	0.1328	0.2928	1.0000[e]
1.0000[f]	1.0000[f]	1.0000[f]	1.0000[f]	

[a] This is a typical case. The procedures used for this comparison are discussed in Appendix B.

[b] The key to the matrix element identification is given in Table X. See also Appendix A, especially Eq. (A5).

[c] The reactance matrix has not been symmetrized and the corresponding transition probabilities are not as accurate as the ones obtained from the symmetrized reactance matrices, which are used throughout this article.

[d] Conservation of particle flux requires that all row and column sums be unity. The sums are carried out before rounding to four significant figures.

[e] Row sum.

[f] Column sum.

[g] See Sec. III.A for description.

instead of as in Eq. (18) of Ref. 32. We now define the matrices $\mathbf{D}(T''\times T'')$ and $\bar{\mathbf{D}}(N''\times T'')$ analogously to $\mathbf{A}$ and $\bar{\mathbf{A}}$; for example, for the symmetric case with $N=N'$ and $T=T'=N+3$, they are given by

$$\begin{aligned} D_{ij}&=D_i^{(j)} && i=1,\cdots,N \\ &=B_i^{(j)} && i=N+1,\cdots,N+3 \\ &=\delta_{i-N-3}^{(j)} && i=N+4,\cdots,2N+3 \\ &=\bar{\beta}_{i-N-3}^{(j)} && i=2N+4,\cdots,2N+6, \qquad \text{(A8)} \\ \bar{D}_{ij}&=\bar{D}_i^{(j)} && i=1,\cdots,N \\ &=\bar{\delta}_{i-N-3}^{(j)} && i=N+1,\cdots,2N. \qquad \text{(A9)} \end{aligned}$$

The reactance matrix is given by

$$\mathbf{R}=\mathbf{V}^{1/2}\bar{\mathbf{D}}\mathbf{D}^{-1}\mathbf{I}^{p}\mathbf{V}^{-1/2}. \qquad \text{(A10)}$$

If the scattering matrix is now computed from the reactance matrix by

$$\mathbf{S}=(\mathbf{1}-i\mathbf{R})^{-1}(\mathbf{1}+i\mathbf{R}), \qquad \text{(A11)}$$

and the reaction probability is computed from the scattering matrix by Eq. (A5), the results will be exactly the same as for the analysis directly in terms of scattering matrix elements. The main advantage of the present scheme lies in the possibility of symmetrizing the $\mathbf{R}$ obtained from (A10) before using (A11). It may sometimes also be considered an advantage that the elements of $\mathbf{R}$ are real.

APPENDIX B

Our accurate results are based on extrapolated probabilities computed from symmetrized reactance matrices as discussed in the text (Sec. III.A). As explained there, these results are believed to be accurate to 2% or better. In general, it is a much weaker criterion to require the symmetry of the probability, reactance or scattering matrices to be within a certain tolerable error limit than to require the accuracy of these matrices within the same limit. Nevertheless, the symmetry of these matrices is a widely used and necessary criterion of accuracy. Our probability matrices automatically satisfy the symmetry criterion because of the method we used to evaluate them. To facilitate comparison of our results with the commonly used accuracy criteria, we present in Table IX a typical case for the extrapolated (unsymmetrized) reactance matrix, scattering matrix, and probability matrix (see also Table X). For this comparison, the scattering matrix is calculated directly from the wavefunction (by a procedure equivalent to that used by Diestler and McKoy) rather than from the reactance matrix. In addition, we give the extrapolated probability matrix according to the symmetrized reactance matrix method used in this paper. The results are extrapolated from calculations using 2025, 3025, and 4225 grid points. For each calculation we used 10 linearly independent numerical solutions in terms of which the wavefunction was expanded, corresponding to two open plus three closed channels for the reagents and equal numbers for the products. The first three matrices of Table IX are symmetric within 3% or better. This compares favorably with the results reported by Miller and Light.[6] Their reflection probability matrix should have been symmetric but the symmetry was not obtained; the asymmetry in the tables they presented varied from 44% to a factor of 178. For the unsymmetrized probability matrix of Table IX, conservation of particle flux is satisfied to 3%. The probabilities from the symmetrized reactance matrix method adopted in this paper satisfy symmetry and conservation of particle flux automatically, as demonstrated by the fourth matrix in Table IX. The difference between any pair of corresponding elements of these two matrices is less than 0.02, and for most pairs less than 0.01.

TABLE X. Table of channel labels (row or column) defining notation for matrix elements of Table IX. Numbers in parentheses after each molecule designate the vibrational quantum numbers.

Label	Channel
1	A+BC(0)
2	A+BC(1)
3	AB(0)+C
4	AB(1)+C

* Supported in part by the United States Atomic Energy Commission, Report Code CALT-767P4-84.

† Present address: Department of Chemistry, University of Minnesota, Minneapolis, Minn. 55455.

‡ Contribution No. 4334.

[1] E. M. Mortensen and K. S. Pitzer, Chem. Soc. (London), Spec. Publ. **16**, 57 (1962).
[2] E. M. Mortensen, J. Chem. Phys. **48**, 4029 (1968).
[3] E. M. Mortensen and L. D. Gucwa, J. Chem. Phys. **51**, 5695 (1969).
[4] D. G. Truhlar and A. Kuppermann, J. Chem. Phys. **52**, 3841 (1970). This reference is a preliminary communication of part of the present work.
[5] D. J. Diestler, J. Chem. Phys. **54**, 4547 (1971).
[6] G. Miller and J. C. Light, J. Chem. Phys. **54**, 1643 (1971).
[7] E. A. McCullough, Jr. and R. E. Wyatt, J. Chem. Phys. **51**, 1253 (1969); **54**, 3578, 3592 (1971).
[8] H. Pelzer and E. Wigner, Z. Physik. Chem. **B15**, 445 (1932); E. Wigner, *ibid.* **B19**, 203 (1932).
[9] H. Eyring, J. Chem. Phys. **3**, 107 (1935).
[10] J. O. Hirschfelder, H. Eyring, and B. Topley, J. Chem. Phys. **4**, 170 (1936).
[11] L. Farkas and E. Wigner, Trans. Faraday Soc. **32**, 708 (1936).
[12] S. Glasstone, K. J. Laidler, and H. Eyring, *The Theory of Rate Processes* (McGraw-Hill, New York, 1941).
[13] R. Weston, J. Chem. Phys. **31**, 892 (1959).
[14] I. Shavitt, J. Chem. Phys. **31**, 1359 (1959).
[15] H. S. Johnston and D. Rapp, J. Am. Chem. Soc. **83**, 1 (1961).
[16] H. S. Johnston, *Gas Phase Reaction Rate Theory* (Ronald, New York, 1966).
[17] A. A. Westenberg and N. de Haas, J. Chem. Phys. **47**, 1393 (1967).
[18] D. J. LeRoy, B. A. Ridley, and K. A. Quickert, Discussions Faraday Soc. **44**, 92 (1968).

[19] I. Schavitt, J. Chem. Phys. **49,** 4048 (1968).
[20] K. A. Quickert and D. J. LeRoy, J. Chem. Phys. **53,** 1325 (1970); **54,** 5444 (1971).
[21] J. Lin and J. C. Light, J. Chem. Phys. **45,** 2545 (1966).
[22] R. A. Marcus, J. Chem. Phys. **45,** 2630 (1966).
[23] R. A. Marcus, J. Chem. Phys. **43,** 1598 (1965).
[24] R. A. Marcus, J. Chem. Phys. **45,** 4493 (1966).
[25] R. A. Marcus, J. Chem. Phys. **46,** 959 (1967). In this article references to earlier treatments assuming vibrational adiabaticity are given.
[26] R. A. Marcus, J. Chem. Phys. **49,** 2617 (1969).
[27] D. G. Truhlar, J. Chem. Phys. **53,** 2041 (1970).
[28] M. Karplus and K. T. Tang, Discussions Faraday Soc. **44,** 56 (1968).
[29] I. Shavitt, R. M. Stevens, F. L. Minn, and M. Karplus, J. Chem. Phys. **48,** 2700 (1968). See errata in Ref. 19.
[30] A. Dalgarno, R. J. W. Henry, and C. S. Roberts, Proc. Phys. Soc. (London) **88,** 611 (1966).
[31] F. T. Wall and R. N. Porter, J. Chem. Phys. **36,** 3256 (1962). The equations in this article are inappropriate for the region where all three internuclear distances are large. Although this region is unimportant in the present article, we modified the equations in an obvious way to correct this deficiency.
[32] D. J. Diestler and V. McKoy, J. Chem. Phys. **48,** 2951 (1968).
[33] D. J. Diestler, J. Chem. Phys. **50,** 4746 (1969).
[34] C. C. Rankin and J. C. Light, J. Chem. Phys. **51,** 1701 (1969).
[35] D. J. Wilson, J. Chem. Phys. **51,** 5008 (1969).
[36] A. J. Taylor and P. G. Burke, Proc. Phys. Soc. (London) **92,** 336 (1967); W. H. Miller, J. Chem. Phys. **50,** 407 (1969); Y. Hahn, Phys. Letters **30B,** 595 (1969). See also H. C. Volkin, Ann. Phys. (N.Y.) **46,** 453 (1968).
[37] T. G. Efimenko, B. N. Zakhariev, and V. P. Zhigunov, Ann. Phys. (N.Y.) **47,** 275 (1968); R. K. Nesbet, Phys. Rev. **179,** 60 (1969); P. Heiss and H. H. Hackenbroich, Z. Physik **235,** 422 (1970).
[38] D. J. Kouri, J. Chem. Phys. **51,** 5204 (1969); M. Baer and D. J. Kouri, J. Chem. Phys. (to be published).
[39] See, e.g., L. Fox, in *Numerical Solution of Ordinary and Partial Differential Equations*, edited by L. Fox (Pergamon, Oxford, 1962), p. 270.
[40] See, e.g., J. Todd, *Survey of Numerical Analysis* (McGraw-Hill, New York, 1962), p. 86.
[41] N. S. F. Mott and H. S. W. Massey, *The Theory of Atomic Collisions* (Clarendon, Oxford, 1965), 3rd Ed., pp. 369–372.
[42] L. M. Delves, Nuclear Phys. **26,** 136 (1961).
[43] M. A. Eliason and J. O. Hirschfelder, J. Chem. Phys. **30,** 1426 (1959).
[44] R. J. LeRoy, K. A. Quickert, and D. J. LeRoy, Trans. Faraday Soc. **66,** 2997 (1970).
[45] D. G. Truhlar and A. Kuppermann, J. Am. Chem. Soc. **93,** 1840 (1971).
[46] R. E. Wyatt, J. Chem. Phys. **51,** 3489 (1969).
[47] R. A. Marcus, J. Chem. Phys. **41,** 610 (1964).
[48] M. S. Child, Discussions Faraday Soc. **44,** 68 (1968).
[49] A. Tweedale and K. J. Laidler, J. Chem. Phys. **53,** 2045 (1970).
[50] R. A. Marcus, J. Chem. Phys. **41,** 2614 (1964).
[51] R. P. Bell, Trans. Faraday Soc. **55,** 1 (1959).
[52] C. Eckart, Phys. Rev. **35,** 1303 (1930).
[53] K. T. Tang, B. Kleinman, and M. Karplus, J. Chem. Phys. **50,** 1119 (1969).
[54] (a) M. Karplus, R. N. Porter, and R. D. Sharma, J. Chem. Phys. **43,** 3259 (1965); (b) F. T. Wall, L. A. Hiller, Jr., and J. Mazur, J. Chem. Phys. **29,** 255 (1958); **35,** 1284 (1961); F. T. Wall and R. N. Porter, J. Chem. Phys. **39,** 3112 (1963).
[55] W. R. Schulz and D. J. LeRoy, J. Chem. Phys. **42,** 3869 (1965).
[56] B. A. Ridley, W. R. Schulz, and D. J. LeRoy, J. Chem. Phys. **44,** 3344 (1966).
[57] R. D. Present, Proc. Natl. Acad. Sci. U.S. **41,** 415 (1955).
[58] R. B. Bernstein, A. Dalgarno, H. S. W. Massey, and I. C. Percival, Proc. Roy. Soc. **A274,** 417 (1963).
[59] J. C. Light, J. Chem. Phys. **40,** 3221 (1964).
[60] D. G. Truhlar and A. Kuppermann, J. Phys. Chem. **73,** 1722 (1969).
[61] D. A. Micha, Arkiv Fysik **30,** 425, 437 (1965).
[62] K. Takayanagi, Advan. At. Mol. Phys. **1,** 149 (1965).
[63] D. Secrest and B. R. Johnson, J. Chem. Phys. **45,** 4556 (1966).
[64] S.-K. Chan. J. C. Light, and J.-L. Lin, J. Chem. Phys. **49,** 86 (1968).
[65] A. S. Cheung and D. J. Wilson, J. Chem. Phys. **51,** 3448 (1969).
[66] V. P. Gutschick, V. McKoy, and D. J. Diestler, J. Chem. Phys. **52,** 4807 (1970).
[67] W. H. Miller, J. Chem. Phys. **53,** 1949 (1970).
[68] R. A. Marcus, Chem. Phys. Letters **7,** 525 (1970). See also R. D. Levine and B. R. Johnson, Chem. Phys. Letters **7,** 404 (1970).
[69] W. H. Miller, J. Chem. Phys. **53,** 3578 (1970); C. C. Rankin and W. H. Miller (unpublished).
[70] R. A. Marcus, J. Chem. Phys. **53,** 4026 (1971).
[71] E. C. Kemble, *The Fundamental Principles of Quantum Mechanics* (Dover, New York, 1958), p. 112.
[72] D. G. Truhlar and A. Kuppermann, Chem. Phys. Letters **9,** 269 (1971).
[73] J. O. Hirschfelder and E. Wigner, J. Chem. Phys. **7,** 616 (1939).
[74] D. L. Bunker, *Theory of Elementary Gas Reaction Rates* (Pergamon, Oxford, 1966).
[75] R. E. Weston, Science **158,** 332 (1967).
[76] This study involves D. G. Truhlar at the University of Minnesota and John T. Adams and Aron Kuppermann at the California Institute of Technology.